EUROPEAN ORGANIZATION FOR NUCLEAR RESEARCH (CERN)

CERN-EP-2023-090
2023/05/24

CMS-TOP-22-013

Observation of four top quark production in proton-proton collisions at $\sqrt{s} = 13$ TeV

The CMS Collaboration*

Abstract

The observation of the production of four top quarks in proton-proton collisions is reported, based on a data sample collected by the CMS experiment at a center-of-mass energy of 13 TeV in 2016–2018 at the CERN LHC and corresponding to an integrated luminosity of 138 fb^{-1}. Events with two same-sign, three, or four charged leptons (electrons and muons) and additional jets are analyzed. Compared to previous results in these channels, updated identification techniques for charged leptons and jets originating from the hadronization of b quarks, as well as a revised multivariate analysis strategy to distinguish the signal process from the main backgrounds, lead to an improved expected signal significance of 4.9 standard deviations above the background-only hypothesis. Four top quark production is observed with a significance of 5.6 standard deviations, and its cross section is measured to be $17.7\,^{+3.7}_{-3.5}\,\text{(stat)}\,^{+2.3}_{-1.9}\,\text{(syst)}$ fb, in agreement with the available standard model predictions.

Submitted to Physics Letters B

*See Appendix B for the list of collaboration members

1 Introduction

Four top quark ($\mathrm{t\bar{t}t\bar{t}}$) production in proton-proton (pp) collisions is among the rarest standard model (SM) processes currently accessible at hadron colliders. While the production occurs predominantly through the strong interaction [1–3], nonnegligible contributions arise also from electroweak (EW) processes [4–6]. Example leading-order (LO) Feynman diagrams are shown in Fig. 1. The SM cross section is calculated at next-to-LO (NLO) in quantum chromodynamics (QCD) and EW theory, including soft-gluon emission corrections at next-to-leading logarithmic accuracy, to be $13.4\,^{+1.0}_{-1.8}$ fb at $\sqrt{s} = 13$ TeV [6]. The quoted uncertainty is from scale variations and the parton distribution functions (PDFs).

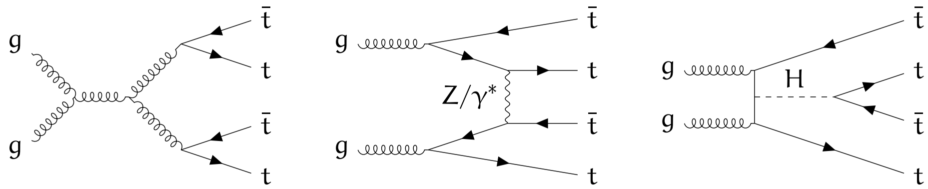

Figure 1: Examples of Feynman diagrams that provide important contributions to $\mathrm{t\bar{t}t\bar{t}}$ production. The first diagram (left) involves only the strong interaction, while the other two involve both strong and electroweak interactions with the exchange of a Z boson or virtual photon (middle), or a Higgs boson (right).

Due to EW contributions involving the exchange of a Higgs boson (H), as shown in Fig. 1 (right), the measurement of the $\mathrm{t\bar{t}t\bar{t}}$ production cross section provides a way to measure the top quark Yukawa coupling [7, 8], complementary to its extraction from measurements of Higgs boson production in association with a top quark pair ($\mathrm{t\bar{t}}$) [9] or $\mathrm{t\bar{t}}$ cross section measurements [10, 11]. The $\mathrm{t\bar{t}t\bar{t}}$ production process is also of interest as a probe for new physics. Many models of physics beyond the SM (BSM) introduce an extension of the Higgs sector, resulting in additional scalar particles that have Yukawa-like interactions with top quarks. Such new particles would enhance the $\mathrm{t\bar{t}t\bar{t}}$ production cross section [12–15]. Supersymmetric extensions of the SM predict new heavy, strongly interacting particles that can decay to top quarks, leading to $\mathrm{t\bar{t}t\bar{t}}$ production via intermediate supersymmetric particles [16–22]. Other BSM scenarios are predicted to affect $\mathrm{t\bar{t}t\bar{t}}$ production as well [23–25], and model-independent evaluations of modifications to the SM in an effective field theory setup have shown the importance of $\mathrm{t\bar{t}t\bar{t}}$ production measurements to constrain these [26–33].

The ATLAS [34] and CMS [35] Collaborations at the CERN LHC performed searches for $\mathrm{t\bar{t}t\bar{t}}$ production using the pp collision data recorded between 2015 and 2018, corresponding to an integrated luminosity of about 140 fb^{-1} and covering the decay channels with zero to four electrons and/or muons (in the following referred to as “leptons”) [36–45]. The dilepton channel is further divided into events where the charge of the two leptons has the same or opposite sign (in the following referred to as same- or opposite-sign lepton pairs, respectively). So far, these searches found evidence for $\mathrm{t\bar{t}t\bar{t}}$ production with a significance of more than three standard deviations (SDs) from the background-only hypothesis [42–44]. However, the observation level of five SDs [46] was not reached. In both experiments, the $\mathrm{t\bar{t}t\bar{t}}$ signal was measured with a significance larger than the expected one, and with a measured cross section higher than the SM prediction [42–44], indicating either statistical fluctuations or an enhancement caused by the presence of BSM physics. Thus, it is of crucial importance to further increase the sensitivity of the $\mathrm{t\bar{t}t\bar{t}}$ measurements.

In this Letter, we present a search for $\mathrm{t\bar{t}t\bar{t}}$ production in events with two same-sign, three, or four leptons, using pp collision data recorded by the CMS experiment in 2016–2018 and corresponding to an integrated luminosity of $138\,\mathrm{fb}^{-1}$. This measurement supersedes the results from Ref. [41] that analyzed events with two same-sign or at least three leptons selected from the same data set and found 2.6 (2.7) SDs of observed (expected) significance for $\mathrm{t\bar{t}t\bar{t}}$ production. Notable improvements, discussed later in this Letter, are achieved in the lepton identification and the tagging of jets originating from the hadronization of bottom (b) quarks, as well as from a revised analysis strategy for the discrimination between signal and background processes based on the application of machine learning techniques. The $\mathrm{t\bar{t}t\bar{t}}$ production cross section $\sigma(\mathrm{t\bar{t}t\bar{t}})$ is extracted with a profile likelihood fit to distributions that provide optimal signal-to-background discrimination. The backgrounds of $\mathrm{t\bar{t}}$ production in association with a W or Z boson ($\mathrm{t\bar{t}W}$ and $\mathrm{t\bar{t}Z}$, respectively) are estimated with free normalization parameters in the fit. The aforementioned improvements increase the sensitivity of the analysis and allow for the observation of the $\mathrm{t\bar{t}t\bar{t}}$ production process with a statistical significance above five SDs. When this Letter was in the final stages of preparation, the ATLAS Collaboration also reported the observation of $\mathrm{t\bar{t}t\bar{t}}$ production [47] with an observed (expected) significance of 6.1 (4.3) SDs.

Tabulated results are provided in the HEPData record for this analysis [48].

2 The CMS detector and event reconstruction

The central feature of the CMS apparatus is a superconducting solenoid of 6 m internal diameter, providing a magnetic field of 3.8 T. Within the solenoid volume are a silicon pixel and strip tracker, a lead tungstate crystal electromagnetic calorimeter (ECAL), and a brass and scintillator hadron calorimeter, each composed of a barrel and two endcap sections. Forward calorimeters extend the pseudorapidity (η) coverage provided by the barrel and endcap detectors. Muons are measured in gas-ionization detectors embedded in the steel flux-return yoke outside the solenoid. A more detailed description of the CMS detector, together with a definition of the coordinate system used and the relevant kinematic variables, can be found in Ref. [35].

Events of interest are selected using a two-tiered trigger system. The first level, composed of custom hardware processors, uses information from the calorimeters and muon detectors to select events at a rate of around 100 kHz within a fixed latency of about 4 μs [49]. The second level, known as the high-level trigger, consists of a farm of processors running a version of the full event reconstruction software optimized for fast processing, and reduces the event rate to around 1 kHz before data storage [50].

A global particle-flow (PF) algorithm [51] aims to reconstruct and identify each individual particle in an event, with an optimized combination of information from the various elements of the CMS detector. The primary vertex (PV) is taken to be the vertex corresponding to the hardest scattering in the event, as described in Section 9.4.1 of Ref. [52]. The energy of photons is obtained from the ECAL measurement. The energy of electrons is obtained from a combination of the electron momentum at the PV as determined by the tracker, the energy of the corresponding ECAL cluster, and the energy sum of all bremsstrahlung photons spatially compatible with originating from the electron track. The energy of muons is obtained from the curvature of the corresponding track. The energy of charged hadrons is determined from a combination of their momentum measured in the tracker and the matching calorimeter energy deposits, corrected for the response function of the calorimeters to hadronic showers. Finally, the energy of neutral hadrons is obtained from the corresponding corrected calorimeter energies.

Hadronic jets are clustered from the PF objects using the infrared- and collinear-safe anti-k_T algorithm [53, 54] with a distance parameter of 0.4. Jet momentum is determined as the vectorial sum of all PF object momenta in the jet, and is found from simulation to be, on average, within

5–10% of the true momentum over the entire transverse momentum (p_T) spectrum and detector acceptance. Additional pp interactions within the same or nearby bunch crossings (pileup) can contribute additional tracks and calorimetric energy depositions, increasing the apparent jet momentum. To mitigate this effect, charged PF objects identified to be originating from pileup vertices are discarded and an offset correction is applied to correct for remaining contributions. Jet energy corrections are derived from simulation studies so that the average measured energy of jets becomes identical to that of particle-level jets. In situ measurements of the momentum balance in dijet, photon+jet, Z+jet, and multijet events are used to determine any residual differences between the jet energy scale (JES) in data and simulation, and appropriate corrections are made. The jet energy resolution (JER) amounts typically to 15–20% at 30 GeV, 10% at 100 GeV, and 5% at 1 TeV. A smearing procedure is applied to match the JER in simulation to that in data [55]. Additional selection criteria are applied to each jet to remove jets potentially dominated by instrumental effects or reconstruction failures. We retain jets for further analysis if they have $p_T > 25\,\text{GeV}$ and $|\eta| < 2.4$, and are separated by $\Delta R = \sqrt{(\Delta\eta)^2 + (\Delta\phi)^2} > 0.4$ from any identified lepton, where $\Delta\eta$ and $\Delta\phi$ are the η and azimuthal angle differences between the jet and lepton directions.

The missing transverse momentum vector $\vec{p}_T^{\text{miss}}$ is computed as the negative vector sum of the $\vec{p}_T$ of all the PF objects in an event, including unclustered energy from the PF objects not associated with any reconstructed lepton, photon, or jet [56]. Its magnitude is denoted as p_T^{miss}. The $\vec{p}_T^{\text{miss}}$ is modified to account for corrections to the energy scale of the reconstructed jets in the event. Anomalous high-p_T^{miss} events can be due to a variety of reconstruction failures, detector malfunctions, or noncollision backgrounds. Such events are rejected by event filters that are designed to identify more than 85–90% of the spurious high-p_T^{miss} events with a mistagging rate less than 0.1% [56].

Jets originating from b quarks are identified with the DEEPJET algorithm [57–59], with three defined working points (WPs) labeled "loose", "medium", and "tight". The loose WP has a selection efficiency for b quark jets of about 90%, and a misidentification rate for c quark (light-quark or gluon) jets of 49 (18)%. Similarly, the efficiencies for b quark, c quark, and light-quark or gluon jets are about 76, 17, and 3% for the medium WP, and 59, 3, and 0.3% for the tight WP. Compared to the DEEPCSV algorithm used in Ref. [41], the b quark jet selection efficiency at the same light-quark and gluon jet misidentification rate is 5–25% higher with the DEEPJET algorithm [59]. Unless specified otherwise, the term "b jets" is used to refer to jets that pass the loose WP requirements.

3 Simulated event samples

Simulated event samples of the signal and background processes are generated with Monte Carlo generators and used to determine the $t\bar{t}t\bar{t}$ signal acceptance, estimate most background contributions, and provide training data for the machine-learning discriminants. The $t\bar{t}t\bar{t}$ signal process is simulated at NLO in QCD with the MADGRAPH5_aMC@NLO v2.6.0 program [2, 60]. Background samples for $t\bar{t}$ production in association with a gauge boson (W, Z, γ) or Higgs boson, single top quark production (s channel, Z boson associated, and WZ diboson associated), Z/γ^* production in association with jets (referred to as Z+jets), and WZ, Zγ, WH, and ZH diboson production are simulated at NLO in QCD with MADGRAPH5_aMC@NLO as well. A simulation with MADGRAPH5_aMC@NLO at LO is performed for $t\bar{t}$ production in association with two bosons, three top quark production ($t\bar{t}t\bar{q}$, $t\bar{t}\bar{t}q$, $t\bar{t}tW$, and $t\bar{t}\bar{t}W$, labeled as ttt), single top quark production in association with a Higgs boson, and same-sign WW diboson production. The POWHEG v2 program [61–69] is used for the simulation of $t\bar{t}$ production, single top quark production (t channel and W boson associated), quark-antiquark-initiated ZZ and opposite-sign WW diboson production, and Higgs boson production via gluon and vector boson fusion at NLO in QCD. The gluon-gluon-initiated ZZ diboson production process is simulated with the MCFM v7.0.1 generator [70–72] at LO in QCD.

The NNPDF3.1NNLO [73] PDFs are used in the matrix-element calculation of all processes. The simulation of parton showering, hadronization, and underlying event is performed with the PYTHIA v8.230 program [74] using the CP5 tune [75]. Double counting of partons generated with MADGRAPH5_aMC@NLO and PYTHIA is eliminated with the FxFx [76] (MLM [77]) matching scheme for NLO (LO) samples. In POWHEG samples, the Higgs boson decay to four leptons is simulated with the JHUGEN v5.2.5 program [78]. Pileup collisions are overlayed to each simulated event, and the generated distribution of the number of events per bunch crossing is matched to that observed in data. All simulated events are processed with a full simulation of the CMS detector based on the GEANT4 toolkit [79].

4 Lepton selection

Electrons are reconstructed via a combination of tracker and ECAL measurements [80, 81] in the range $|\eta| < 2.5$, and electrons in the barrel–endcap transition region $1.44 < |\eta| < 1.57$ are removed because of the not optimal electron reconstruction in this region. The curvature of the electron track is evaluated with three different methods to estimate the electron charge, and we require all three charge evaluations to agree for each selected electron, thereby reducing the background from charge mismeasurements (referred to as "charge misID") by a factor of five with an efficiency of about 97% [82]. Muons are reconstructed in the range $|\eta| < 2.4$ by combining information from the tracker, the muon spectrometers, and the calorimeters in a global fit [83]. The charge mismeasurements of muons are negligible [84, 85].

We select electrons and muons with $p_{\mathrm{T}} > 10\,\mathrm{GeV}$ and require that they are compatible with originating from the PV and fulfill a loose set of identification (ID) criteria [80, 83]. The relative isolation I_{rel} of a lepton is defined as the scalar p_{T} sum of all particles within a certain distance ΔR around the lepton, divided by the lepton p_{T}. We use a p_{T}-dependent distance [86] of $\Delta R < 0.2$ for leptons with $p_{\mathrm{T}} < 50\,\mathrm{GeV}$, $\Delta R < 10\,\mathrm{GeV}/p_{\mathrm{T}}$ for $50 < p_{\mathrm{T}} < 200\,\mathrm{GeV}$, and $\Delta R < 0.05$ for $p_{\mathrm{T}} > 200\,\mathrm{GeV}$, and require all leptons to have $I_{\mathrm{rel}} < 0.4$.

To distinguish leptons originating directly from the prompt decay of top quarks or massive bosons (prompt leptons) from both genuine leptons produced in hadron decays and photon conversions or jet constituents misidentified as leptons (nonprompt leptons), we employ gradient boosted decision trees (BDTs) trained with the XGBOOST program [87], following the methods developed for various CMS measurements and searches with multilepton signatures [9, 88–92]. Simulated $\mathrm{t\bar{t}t\bar{t}}$, $\mathrm{t\bar{t}W}$, $\mathrm{t\bar{t}Z}$, $\mathrm{t\bar{t}H}$, and tZq ($\mathrm{t\bar{t}}$) samples are used to provide the prompt-lepton (nonprompt-lepton) training data. The input variables for the BDTs are the lepton p_{T} and $|\eta|$, isolation information, variables quantifying the consistency of the lepton track with the PV, and properties of the nearest jet defined as the jet that includes the PF particle corresponding to the reconstructed lepton. For electrons, the multivariate discriminant from Ref. [80] is used as additional input. For muons, an additional input is the segment compatibility defined in Ref. [83]. Besides the lepton p_{T}, the most important input variables are the ratio of the lepton p_{T} to the nearest jet p_{T} and the DEEPJET score of the nearest jet, and also the multivariate discriminant in the case of the electron BDT. A dedicated study of the BDT strategy applied here with the full list of input variables is presented in Ref. [93] for the case of muons.

We define two sets of lepton ID criteria labeled "loose" and "tight". Electrons and muons pass the tight ID if their BDT discriminant value is above a certain threshold. The efficiencies of this selection are shown in Fig. 2, and compared to the efficiencies of the ID criteria used in Ref. [41]. To compensate for larger background contributions from nonprompt electrons compared to those from nonprompt muons, the threshold for tight electrons is set at a lower misidentification probability for nonprompt leptons, resulting also in a smaller prompt-lepton efficiency. The loose ID is defined by requiring leptons to either pass the tight ID or a set of requirements on the p_T ratio and the nearest jet DEEPJET score.

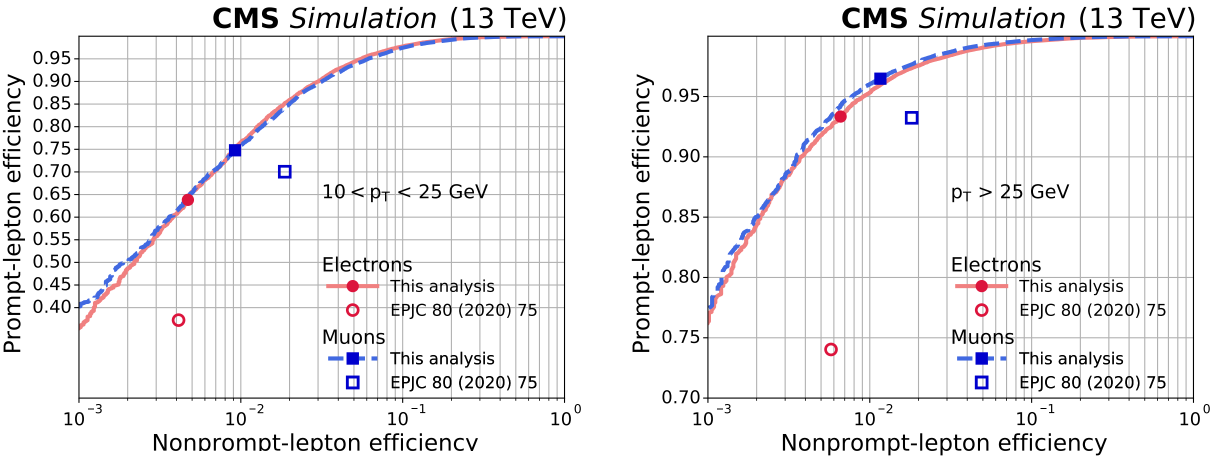

Figure 2: Efficiency of selecting prompt leptons as a function of the misidentification probability for nonprompt leptons evaluated in simulated $t\bar{t}$ events for the electron (red solid line) and muon (blue dashed line) ID BDT, shown for leptons with $10 < p_T < 25$ GeV (left) and $p_T > 25$ GeV (right). Indicated with filled markers are the efficiencies for the ID criteria applied in this measurement and with empty markers those for the ID criteria applied in Ref. [41], where red circles and blue squares are used for electron and muon criteria, respectively.

5 Event selection and search strategy

The analyzed event sample is collected with a combination of triggers that require the presence of one, two, or three leptons. Events must contain between two and four loose leptons, with $p_T > 25$ and 20 GeV for the highest p_T (leading) and second-highest p_T (subleading) lepton, and at least two jets, of which at least one is identified as b jet. Events with two (three and four) leptons are removed if any lepton pair has an invariant mass below 20 (12) GeV, to reduce backgrounds from leptonic decays of low-mass resonances. Signal regions (SRs) and control regions (CRs) are defined using events in which all leptons pass the tight ID criteria, whereas events with at least one loose but not tight lepton are used as a sideband for the nonprompt-lepton background estimation. In events with two leptons, the SRs and CRs additionally require both leptons to have the same sign, and events with opposite-sign leptons are used as a sideband for the estimation of the charge-misID background. In events with four leptons, we additionally require the sum of the lepton charges to be zero. For the SR and CR definitions, the number of jets and b jets (N_j and N_b), the scalar p_T sum of all jets (H_T), and the invariant mass $m(\ell\ell)$ of opposite-sign same-flavor (OSSF) lepton pairs are used. A schematic representation of the SR and CR definitions is shown in Fig. 3.

For the events with two same-sign leptons (2ℓ channel), the SR-2ℓ is defined by $N_j \geq 4$, $N_b \geq 2$, and $H_T > 280$ GeV, and additionally either $N_j \geq 6$ or $N_b \geq 3$. The CR-2ℓ-45j2b, enriched in $t\bar{t}W$ production, comprises all events with $4 \leq N_j \leq 5$, $N_b = 2$, and $H_T > 280$ GeV. The CR-2ℓ-23j1b, used to constrain both $t\bar{t}W$ production and nonprompt-lepton backgrounds, is

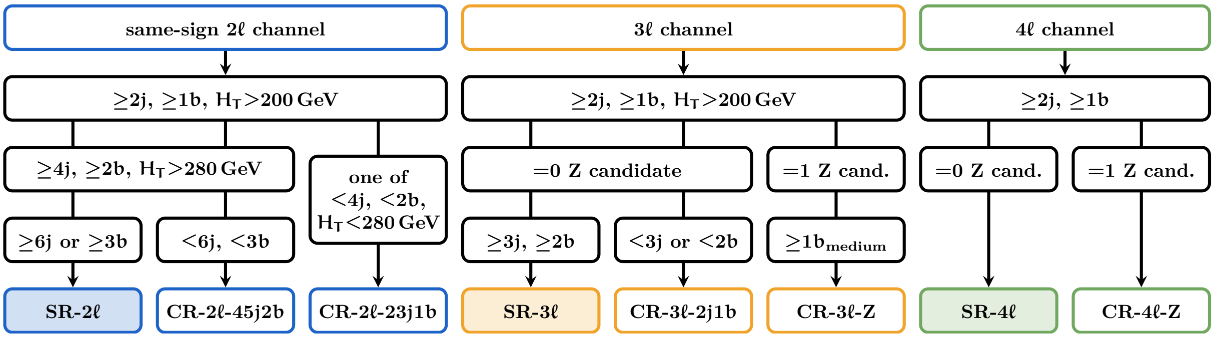

Figure 3: Schematic representation of the event selection and categorization.

defined by all events with $H_T > 200\,\text{GeV}$ that fail exactly one of the requirements $N_j \geq 4$, $N_b \geq 2$, or $H_T > 280\,\text{GeV}$.

The SR-3ℓ for events with three leptons (3ℓ channel) is defined by $N_j \geq 3$, $N_b \geq 2$, $H_T > 200\,\text{GeV}$, and the requirement that there is no OSSF lepton pair with $|m(\ell\ell) - m_Z| < 15\,\text{GeV}$ (referred to as "Z candidate"). The last requirement, which uses the world-average Z boson mass [94], rejects events consistent with leptonically decaying Z bosons. The CR-3ℓ-2j1b, used to constrain nonprompt-lepton backgrounds, consists of events that pass the SR-3ℓ requirements except that they have $N_j = 2$ or $N_b = 1$. To constrain $\mathrm{t\bar{t}Z}$ production, the CR-3ℓ-Z is defined by requiring $H_T > 200\,\text{GeV}$, the presence of a Z candidate, and that at least one jet passes the medium DeepJet WP.

No additional jet requirements are imposed on events with four leptons (4ℓ channel). Events that have no Z candidate form the SR-4ℓ, while events with exactly one Z candidate form the CR-4ℓ-Z enriched in $\mathrm{t\bar{t}Z}$ production.

To enhance the separation of signal events and those from different background processes, we employ multiclassification BDTs trained with the TMVA program [95]. The BDTs provide output scores for three classes of events: the $\mathrm{t\bar{t}t\bar{t}}$ signal, associated $\mathrm{t\bar{t}}$ production with a heavy boson ($\mathrm{t\bar{t}Z}$, $\mathrm{t\bar{t}W}$, and $\mathrm{t\bar{t}H}$, referred to as $\mathrm{t\bar{t}X}$), and $\mathrm{t\bar{t}}$ production, which is the dominant contribution to the nonprompt-lepton and charge-misID backgrounds. Simulated event samples of $\mathrm{t\bar{t}t\bar{t}}$, $\mathrm{t\bar{t}Z}$, $\mathrm{t\bar{t}W}$, $\mathrm{t\bar{t}H}$, and $\mathrm{t\bar{t}}$ production are used in the training. Kinematic differences and different background compositions motivate separate BDT trainings per decay channel, but sufficient simulated events in the training samples are required as well. Since the size of the available 4ℓ samples is limited, we train one BDT for the combined 3ℓ+4ℓ channel and a second one for the 2ℓ channel.

The variables used in the BDT training are listed in Table 1. The 3ℓ+4ℓ channels have at most one hadronically decaying top quark and thus we use more observables related to the reconstruction of W bosons and top quarks from leptons and p_T^{miss}, while the 2ℓ channel has two hadronically decaying top quarks and we use specific observables targeting the reconstruction of both. The modeling of each input variable in the simulated samples is validated in data. The BDT scores can be interpreted as measures of how likely an event is to originate from the corresponding classes, and good agreement between simulation and data is found for the shapes of their distributions in the CRs.

Events selected in the SRs are further split according to the class that yields the highest BDT score, resulting in "$\mathrm{t\bar{t}t\bar{t}}$-like", "$\mathrm{t\bar{t}X}$-like", and "$\mathrm{t\bar{t}}$-like" SR classes. These SR classes, together with the CRs, are separate inputs to the fit for the cross section extraction. Due to the low number of events, the $\mathrm{t\bar{t}}$ class is added to the $\mathrm{t\bar{t}X}$ class in SR-4ℓ.

Table 1: List of the input variables to the event multiclassification BDTs. The last two columns indicate the importance rank of the observables in the 2ℓ and 3ℓ+4ℓ BDT trainings, respectively, and a dash indicates that the observable is not used in that training. The m_{T2} variable, defined in Refs. [96, 97], is constructed from $\vec{p}_{\mathrm{T}}^{\text{miss}}$ and two four-momenta of the particles or particle systems specified in the table.

Symbol	Definition	2ℓ	3ℓ+4ℓ
$\max_2$ DJ	Second-highest DEEPJET score of any jet	1	1
$\max_3$ DJ	Third-highest DEEPJET score of any jet	8	15
$\max_4$ DJ	Fourth-highest DEEPJET score of any jet	29	—
$\mathrm{DJ}(\mathrm{j}_1)$	DEEPJET score of leading jet	9	7
$\mathrm{DJ}(\mathrm{j}_2)$	DEEPJET score of subleading jet	12	11
$\mathrm{DJ}(\mathrm{j}_3)$	DEEPJET score of jet with third-highest p_{T}	16	18
$\mathrm{DJ}(\mathrm{j}_4)$	DEEPJET score of jet with fourth-highest p_{T}	—	22
$\Delta R(\ell_1, \ell_2)$	ΔR between leading and subleading lepton	2	4
$\Delta\phi(\ell_1, \ell_2)$	$\Delta\phi$ between leading and subleading lepton	5	—
$\min \Delta R(\mathrm{b}, \mathrm{b})$	Smallest ΔR between any two b jets	3	3
$\min \Delta R(\ell, \mathrm{b})$	Smallest ΔR between any lepton and b jet	6	—
$\min_2 \Delta R(\ell, \mathrm{b})$	Second-smallest ΔR between any lepton and b jet	4	6
$m(\mathrm{t}_1)$	Invariant mass of any three jets, of which one is identified as b jet, that is closest to the top quark mass	7	2
$m(\mathrm{W}_1)$	Invariant mass of any two jets used for $m(\mathrm{t}_1)$ that is closest to the W boson mass	10	5
$m(\mathrm{t}_2)$	Invariant mass of any three jets, of which one is identified as b jet and none of which is used for $m(\mathrm{t}_1)$, that is closest to the top quark mass	23	—
$m(\mathrm{W}_2)$	Invariant mass of any two jets used for $m(\mathrm{t}_2)$ that is closest to the W boson mass	28	—
H_{T}	Scalar p_{T} sum of all jets	14	8
$p_{\mathrm{T}}^{\text{miss}}$	Missing transverse momentum	20	13
N_{j}	Number of jets	24	23
$N_{\mathrm{b}}^{\text{tight}}$	Number of jets passing the tight DEEPJET WP	27	24
$N_{\mathrm{b}}^{\text{medium}}$	Number of jets passing the medium DEEPJET WP	30	—
$p_{\mathrm{T}}(\ell_1)$	Highest p_{T} of any lepton	19	14
$p_{\mathrm{T}}(\ell_2)$	Second-highest p_{T} of any lepton	15	17
$p_{\mathrm{T}}(\ell_3)$	Third-highest p_{T} of any lepton	—	9
$p_{\mathrm{T}}(\mathrm{j}_1)$	Highest p_{T} of any jet	18	12
$p_{\mathrm{T}}(\mathrm{j}_2)$	Second-highest p_{T} of any jet	22	—
$p_{\mathrm{T}}(\mathrm{j}_3)$	Third-highest p_{T} of any jet	—	10
$p_{\mathrm{T}}(\mathrm{j}_4)$	Fourth-highest p_{T} of any jet	11	—
$p_{\mathrm{T}}(\mathrm{j}_5)$	Fifth-highest p_{T} of any jet	13	21
$m_{\mathrm{T}}(\ell_1)$	Transverse mass of leading lepton and $p_{\mathrm{T}}^{\text{miss}}$	17	19
$m_{\mathrm{T}}(\ell_2)$	Transverse mass of subleading lepton and $p_{\mathrm{T}}^{\text{miss}}$	21	16
$m_{\mathrm{T2}}(\ell)$	m_{T2} variable constructed from leading and subleading leptons	—	20
$m_{\mathrm{T2}}(\mathrm{b})$	m_{T2} variable constructed from leading and subleading b jets	25	—
$m_{\mathrm{T2}}(\ell+\mathrm{b})$	m_{T2} variable constructed from two lepton+jet systems built with leading two leptons and leading two b jets	26	—

The approach followed here is different from the BDT approach of Ref. [41] in several aspects. We train separate BDTs for the 2ℓ and 3ℓ+4ℓ channels, with an extended set of input variables separately optimized for the two channels. Especially the usage of DEEPJET discriminants of several jets and ΔR information between leptons and b jets, which were not used in Ref. [41], improves the sensitivity of our BDTs, as indicated by the high importance ranking of these observables shown in Table 1. The performance also benefits from looser requirements in the initial event selection, allowing an improvement of the BDTs with respect to the sensitivity achieved by a series of tight one-dimensional selections. Finally, the setup as a multiclassifier that simultaneously separates two characteristically different background classes facilitates a good separation of processes, and the use of all output classes in the fit improves the constraints on the main background contributions.

6 Background estimation

Background contributions to the SRs are categorized into processes in which all selected leptons are prompt (prompt background) and processes with at least one nonprompt lepton (nonprompt background). In the 2ℓ channel, we additionally separate prompt-background contributions from the charge-misID backgrounds. Prompt backgrounds are estimated from the simulated samples described in Section 3, while nonprompt and charge-misID backgrounds are estimated from sideband samples in data. All predictions from simulation are normalized according to the measured integrated luminosity and state-of-the-art cross section predictions.

Prompt-background contributions with top quarks are grouped into $\mathrm{t\bar{t}X}$, ttt, and other associated top quark production processes labeled "other t". Contributions from $\mathrm{t\bar{t}}$ production, including $\mathrm{t\bar{t}b\bar{b}}$ and other contributions with additional jets, do not contribute to the prompt background as they either need to have a charge-misID lepton or an additional nonprompt lepton to pass the event selection. Instead, these processes are the dominant contributions to the nonprompt and charge-misID backgrounds. Prompt-background contributions without top quarks are mainly due to the production of two or three heavy vector bosons, grouped together as "VV(V)", where the leptons are from leptonic boson decays and the jets originate mostly from additional QCD radiation. Contributions with photon conversions, both in processes with top quarks and only vector bosons, are grouped together as "Xγ".

The $\mathrm{t\bar{t}W}$ background is relevant in the 2ℓ and 3ℓ channels, $\mathrm{t\bar{t}Z}$ in the 3ℓ and 4ℓ channels with smaller contributions in the 2ℓ channel, and $\mathrm{t\bar{t}H}$ in all channels. The $\mathrm{t\bar{t}W}$ prediction is normalized to a cross section of 722 ± 74 fb [98], $\mathrm{t\bar{t}Z}$ to 859 ± 80 fb [99], and $\mathrm{t\bar{t}H}$ to 504 ± 39 fb [99]. The quoted uncertainties are from scale variations and PDF uncertainties evaluated in the SM cross section calculations, and are different from the normalization uncertainties we consider in our measurement and discuss in Section 7. The contribution from ttt production to the SR $\mathrm{t\bar{t}t\bar{t}}$ classes is predicted to be less than 9% of the $\mathrm{t\bar{t}t\bar{t}}$ yield, but can be important since the kinematic properties are similar to the $\mathrm{t\bar{t}t\bar{t}}$ signal process. We normalize the ttt contribution to a cross section of 2.0 ± 0.3 fb, calculated at NLO in QCD and including LO EW corrections [100]. The contributions in other t are small, with the largest remaining contribution being tZq production, normalized to a cross section of 94.2 ± 3.1 fb for simulated events with $m(\ell\ell) > 30$ GeV [101]. We show the ttt and other t contributions separately in the figures for the SR $\mathrm{t\bar{t}t\bar{t}}$ classes, but merge ttt into other t in all other cases.

The main background contributions in the VV(V) group are WZ production in the 2ℓ and 3ℓ channels, and ZZ production in the 4ℓ channel. The number of additional jets in the predicted WZ and ZZ samples is known to be underestimated [9, 89, 102] and thus studied in two data validation regions. A sample of WZ candidate events in data is selected by requiring three

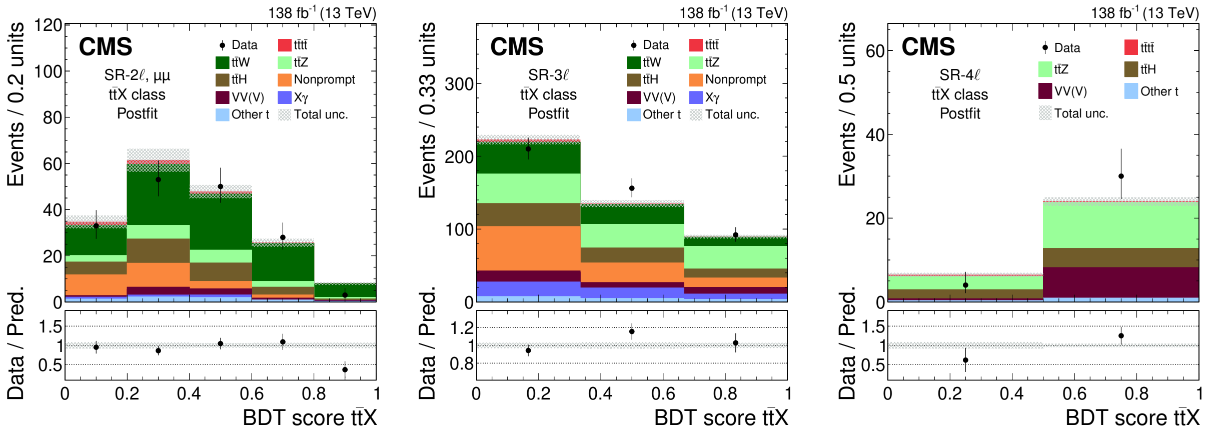

Figure 4: Comparison of the number of observed (points) and predicted (colored histograms) events in the BDT score $\mathrm{t\bar{t}X}$ in the $\mathrm{t\bar{t}X}$ classes of SR-2ℓ in the $\mu\mu$ category (left), of SR-3ℓ (middle), and of SR-4ℓ (right). The vertical bars on the points represent the statistical uncertainties in the data, and the hatched bands the total uncertainty in the predictions. The signal and background yields are shown with their best fit normalizations from the simultaneous fit to the data ("postfit").

leptons, one Z candidate, a three-lepton invariant mass $m(\ell\ell\ell)$ with $|m(\ell\ell\ell) - m_{\mathrm{Z}}| > 15\,\mathrm{GeV}$, $p_{\mathrm{T}}^{\mathrm{miss}} > 30\,\mathrm{GeV}$, and no b jets. More than 70% of the selected events originate from WZ production, with smaller contributions from nonprompt leptons and ZZ production. A sample of ZZ candidate events in data is selected by requiring four leptons that form two Z candidates, and contributions from other processes to this selection are found to be negligible. A disagreement between data and prediction is observed in the jet multiplicity distribution in both samples, and scale factors are derived per N_{j} bin that increase the contribution of WZ (ZZ) production at higher jet multiplicities by factors of up to 2.7 (1.8).

The contributions from the dominant prompt-background processes are treated separately in the fit. Effective constraints are obtained from the inclusion of the SR $\mathrm{t\bar{t}X}$ classes, as well as the CR-3ℓ-Z and CR-4ℓ-Z, in the cross section extraction. Distributions of the BDT score $\mathrm{t\bar{t}X}$ in the SR $\mathrm{t\bar{t}X}$ classes are shown in Fig. 4 for the $\mu\mu$ category of SR-2ℓ, SR-3ℓ, and SR-4ℓ. Jet and b jet multiplicity distributions in the CR-3ℓ-Z and CR-4ℓ-Z are shown in Fig. 5. Due to the high purity of these regions in $\mathrm{t\bar{t}W}$ and $\mathrm{t\bar{t}Z}$ production, we can extract normalization parameters for these processes from the fit without prior constraints.

Nonprompt-background contributions are estimated with a "tight-to-loose" ratio method [103]. The probabilities for a loose lepton to also pass the tight ID are measured, separately for electrons and muons, as functions of p_{T} and $|\eta|$ in a data sample enriched in events composed uniquely of jets produced through the strong interaction, which is rich in nonprompt leptons. The measured probability is then applied to data events in a sideband of the SRs and CRs where one or more of the selected leptons fail the tight ID while passing the loose ID. The method is validated in simulation both with $\mathrm{t\bar{t}}$ and Z+jets production events, separately for nonprompt electrons and muons, as well as in comparison of data and predicted background yields in CR-2ℓ-23j1b, CR-2ℓ-45j2b, and CR-3ℓ-2j1b. In all cases, an agreement of better than 30% is found in the most relevant kinematic distributions, and we assign 30% as a normalization uncertainty to the nonprompt background. The agreement in three different selections enriched in nonprompt-lepton backgrounds is shown in Fig. 6.

To determine the charge-misID background, the electron charge-misID probability is determined in simulated Z+jets samples and parameterized as a function of p_{T} and $|\eta|$. This proba-

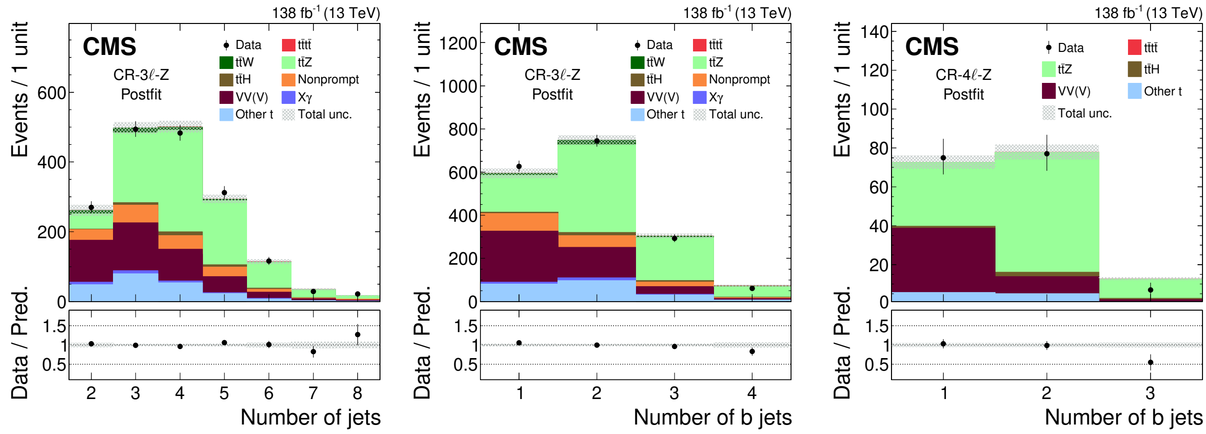

Figure 5: Comparison of the number of observed (points) and predicted (colored histograms) events in the number of jets distribution in CR-3ℓ-Z (left), and in the number of b jets distribution in CR-3ℓ-Z (middle) and CR-4ℓ-Z (right). The vertical bars on the points represent the statistical uncertainties in the data, and the hatched bands the total uncertainty in the predictions. The signal and background yields are shown with their best fit normalizations from the simultaneous fit to the data ("postfit").

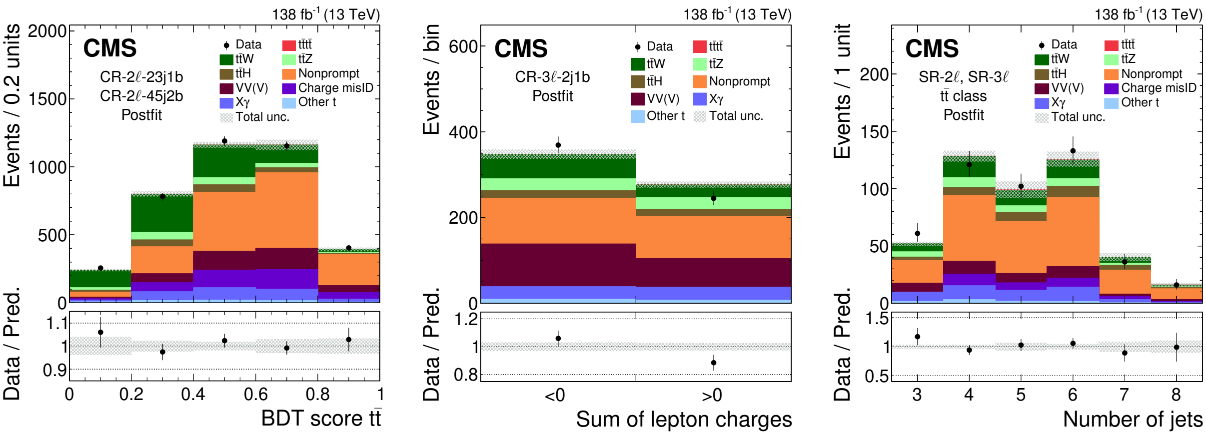

Figure 6: Comparison of the number of observed (points) and predicted (colored histograms) events in the BDT score $t\bar{t}$ in the combined CR-2ℓ-23j1b and CR-2ℓ-45j2b (left), in the event yields with negative and positive sum of lepton charges in CR-3ℓ-2j1b (middle), and in the number of jets distribution in the $t\bar{t}$ class of the combined SR-2ℓ and SR-3ℓ (right). The vertical bars on the points represent the statistical uncertainties in the data, and the hatched bands the total uncertainty in the predictions. The signal and background yields are shown with their best fit normalizations from the simultaneous fit to the data ("postfit").

bility is applied as a scale factor to sideband events in data (i.e., with opposite-sign instead of same-sign leptons) to obtain a prediction of the charge-misID background in the SR-2ℓ. A validation region (its sideband) is defined by requiring exactly two tight same-sign (opposite-sign) electrons that form a Z candidate. To evaluate a possible mismodeling of the charge-misID probability in simulation, we evaluate the ratio of the sideband yields to the validation region yields both in simulation and data, and derive correction factors to the charge-misID probability from the data-to-simulation differences in this ratio. The correction factors are evaluated separately for each year of data taking and integrated over electron p_T and $|\eta|$. After applying the scale and correction factors to the sideband event yields, the agreement with the validation region yields is better than 15% across all relevant kinematic distributions.

7 Systematic uncertainties

Several sources of systematic uncertainty affect the acceptance and reconstruction efficiency in simulation, the background event yields, and the distributions of the observables used for the signal extraction. Experimental uncertainties in the integrated luminosity, lepton selection efficiency, trigger efficiency, JES, b tagging efficiency, and nonprompt-background estimation are considered with several sources each, of which some are correlated and others uncorrelated between the years of data taking. Only the experimental uncertainties from JER and unclustered $p_{\mathrm{T}}^{\mathrm{miss}}$ contributions are fully uncorrelated between the data-taking years. Uncertainties in the simulated pileup distribution, background normalization, and shapes of the fitted observables estimated from simulation are fully correlated between the data-taking years.

The measured integrated luminosity values for the three data-taking years have uncertainties between 1.2 and 2.5% [104–106], while the overall uncertainty for the combined data set is 1.6%, affecting both the background predictions from simulation and the measurement of the $\mathrm{t\bar{t}t\bar{t}}$ cross section. To evaluate the uncertainty in the distribution of pileup events in simulation, we vary the total pp inelastic cross section by $\pm 4.6\%$.

The efficiency of the tight ID selection of electrons and muons is measured in data and simulation with the "tag-and-probe" method in $\mathrm{Z} \to \ell^+\ell^-$ events [107]. Per-lepton correction factors are derived and applied to simulated events, and statistical and systematic uncertainties are considered. The trigger efficiency is measured by selecting events with two or three leptons in an unbiased data sample, collected with triggers on $p_{\mathrm{T}}^{\mathrm{miss}}$ or hadronic activity, and corrections are derived to match the efficiency in simulation to that observed in data. A systematic uncertainty of 3% is assigned to simulated event yields to cover residual differences, and additionally the statistical uncertainties in the measurement are considered. Special correction factors are applied for a gradual shift in the timing of the ECAL inputs to the first-level trigger, which caused a specific trigger inefficiency during the 2016 and 2017 data-taking periods [49].

The JES and JER uncertainties are taken into account by applying variations to the energy of the reconstructed jets in simulated events, considering various uncertainty sources split between detector regions and data-taking years [55]. The JES variations, as well as an additional variation to account for uncertainty contributions from unclustered PF particles [56], are also propagated to the $p_{\mathrm{T}}^{\mathrm{miss}}$. Corrections are applied to simulated events to match the shape of the DEEPJET discriminant in simulation to that in data, and uncertainties in the correction factors are evaluated separately for heavy- and light-flavor or gluon jets [57].

Uncertainties in the background predictions include normalization uncertainties of 7.7% for $\mathrm{t\bar{t}H}$ [99], 6.2% for WZ [108], 20% for ttt [100], 20% for other t [92], 6% for VV(V) [109, 110], and 5% for $\mathrm{X}\gamma$ [111], as well as statistical uncertainties in the N_{j} scale factors applied to the WZ and ZZ backgrounds. The normalization of the $\mathrm{t\bar{t}Z}$ and $\mathrm{t\bar{t}W}$ background contributions are not constrained a priori but treated as free parameters in the fit. For the nonprompt-background prediction, the statistical uncertainties in the measured tight-to-loose ratio and the sideband region yields are considered, as well as an overall normalization uncertainty. Normalization uncertainties in the nonprompt and charge-misID backgrounds are assigned based on the observed agreement in the validation tests discussed in Section 6. For the nonprompt background, the uncertainty of 30% is applied separately for nonprompt electrons and muons, and split into two components of 20% each that are either fully correlated or uncorrelated between the data-taking years, to account both for possible systematic effects in the method itself and for potential year-to-year differences. For the charge-misID background, the statistical uncertainty in the event yields in the sideband regions and a normalization uncertainty of 15% are considered.

Various modeling uncertainties are considered for the signal predictions as well as for all simulated background predictions. The choice of the renormalization and factorization scales in the matrix-element calculations are assessed by individual and simultaneous variations up and down by a factor of 2 (excluding the two extreme variations) [112], and evaluating the envelope of the six obtained variations in the fitted distributions separately for each process. The limited knowledge of the proton PDFs is taken into account using NNPDF replicas [73] and applying the procedure described in Ref. [113], resulting in 100 individual variations that are evaluated simultaneously for all processes. For the choice of the renormalization scale for QCD emissions in initial-state (final-state) radiation in the parton shower simulation, individual variations by a factor of 2 up and down are considered, separately (simultaneously) for the considered processes. The variations associated with the modeling uncertainties generally affect the overall normalization, the simulated acceptance, and the shapes of the fitted distributions. Since background normalization uncertainties are assigned separately and no such uncertainty is required when measuring the cross section of the signal process, we remove the impact on the overall normalization of each process before any selection from these variations.

Additional uncertainties are considered to account for a possible mismodeling in the jet multiplicity in $\mathrm{t\bar{t}X}$ production processes. Motivated by dedicated studies of the cross section ratio of $\mathrm{t\bar{t}}$ production in association with additional b jets and light-flavor or gluon jets [114] that find an underprediction of additional b jets in simulated event samples, we assign a conservative uncertainty of 40% as additional normalization uncertainty to the contributions of $\mathrm{t\bar{t}W}$, $\mathrm{t\bar{t}Z}$, and $\mathrm{t\bar{t}H}$ production with at least one additional b jet at the particle level, uncorrelated between these processes. Dedicated theoretical studies have evaluated the possible mismodeling in the number of additional jets in $\mathrm{t\bar{t}W}$ production [98], and we apply a corresponding additional uncertainty that reweights the N_{j} distribution in $\mathrm{t\bar{t}W}$ production with an increase of up to 55% in 2ℓ events with seven or more jets.

8 Results

The measured cross sections of the $\mathrm{t\bar{t}t\bar{t}}$ signal process and the $\mathrm{t\bar{t}W}$ and $\mathrm{t\bar{t}Z}$ background processes are extracted from a simultaneous binned profile likelihood fit to the data in the SRs and CRs [115, 116]. A binned likelihood function $L(r, \theta)$ is constructed as the product of the Poisson probabilities to obtain the observed yields given the predicted signal and background estimates in each bin, and includes all sources of systematic uncertainty as nuisance parameters. The set r denotes the signal strength modifiers that scale the normalizations of the predicted $\mathrm{t\bar{t}t\bar{t}}$, $\mathrm{t\bar{t}W}$, and $\mathrm{t\bar{t}Z}$ estimates, and the set θ denotes the nuisance parameters. Statistical uncertainties in the predicted yields are implemented through a single nuisance parameter in each bin for all processes [117, 118]. The fitted distributions are the BDT scores in the SR classes, the BDT score $\mathrm{t\bar{t}}$ in CR-2ℓ-23j1b and CR-2ℓ-45j2b, the N_{j} distribution in CR-3ℓ-Z and CR-4ℓ-Z, and the event yields with positive or negative sum of lepton charges in CR-3ℓ-2j1b. In SR-2ℓ, the $\mathrm{t\bar{t}t\bar{t}}$ and $\mathrm{t\bar{t}X}$ classes are also split according to the lepton flavors to achieve a better separation of the nonprompt, charge-misID, and $\mathrm{X}\gamma$ backgrounds. In Fig. 7, the yields in the SR $\mathrm{t\bar{t}t\bar{t}}$ classes after the fit are shown. A comparison of the yields before and after the fit is given in Table 2.

The test statistic $q(r) = -2\ln L(r, \widehat{\theta}_r)/L(\widehat{r}, \widehat{\theta})$ is constructed from the sets $\widehat{r}$ and $\widehat{\theta}$ that simultaneously maximize L, and using the set $\widehat{\theta}_r$ that maximizes L for a fixed set r. We employ a calculation that simplifies $q(r)$ using an asymptotic approximation [115, 116]. The observed (expected) statistical significance of the $\mathrm{t\bar{t}t\bar{t}}$ signal is found to be 5.6 (4.9) SDs from the background-only hypothesis. The results when fitting each channel on its own are summarized in Fig. 8, with the largest sensitivity provided by the 2ℓ channel. This constitutes an observation of $\mathrm{t\bar{t}t\bar{t}}$ pro-

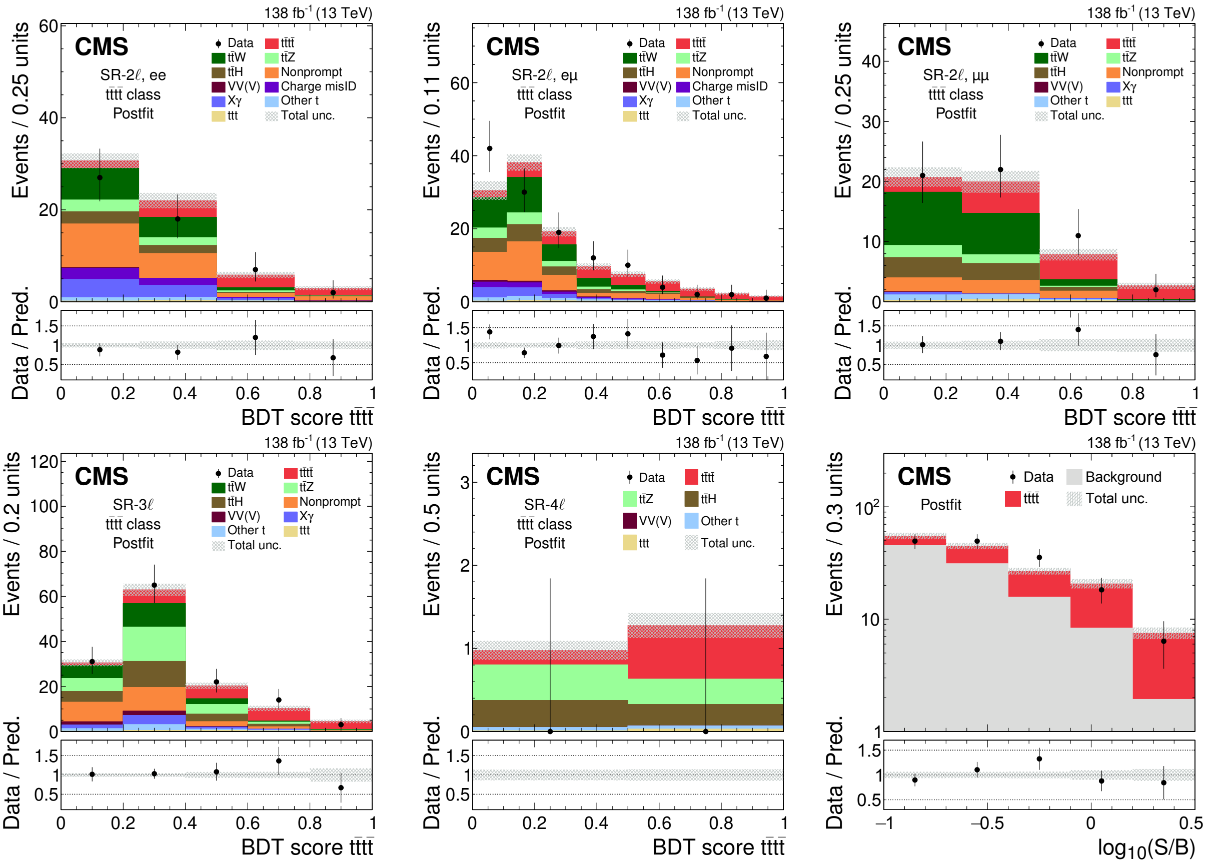

Figure 7: Comparison of the number of observed (points) and predicted (colored histograms) events in the BDT score $\mathrm{t\bar{t}t\bar{t}}$ in the $\mathrm{t\bar{t}t\bar{t}}$ classes of SR-2ℓ, shown for the ee (upper left), eμ (upper middle), and $\mu\mu$ (upper right) categories, of SR-3ℓ (lower left) and of SR-4ℓ (lower middle). Additionally, the comparison is shown for all SRs combined as a function of $\log_{10}(\mathrm{S/B})$ (lower right), where S and B are evaluated for each bin of the fitted distributions as the predicted signal and background yields before the fit to data. Bins with $\log_{10}(\mathrm{S/B}) < -1$ are not included, and bins with $\log_{10}(\mathrm{S/B}) > 0.5$ are included in the last bin. The vertical bars on the points represent the statistical uncertainties in the data, and the hatched bands the total uncertainty in the predictions. The signal and background yields are shown with their best fit normalizations from the simultaneous fit to the data ("postfit").

duction. The cross section of $\mathrm{t\bar{t}t\bar{t}}$ production is measured to be

$$\sigma(\mathrm{t\bar{t}t\bar{t}}) = 17.7\,^{+3.7}_{-3.5}\,(\mathrm{stat})\,^{+2.3}_{-1.9}\,(\mathrm{syst})\,\mathrm{fb} = 17.7\,^{+4.4}_{-4.0}\,\mathrm{fb}.$$

This result is in agreement with the SM prediction of $13.4\,^{+1.0}_{-1.8}$ fb [6] at the level of 1.0 SDs, when taking uncertainties of both prediction and measurement into account.

The measurement of $\sigma(\mathrm{t\bar{t}t\bar{t}})$ is limited by the statistical uncertainty in the SR event yields. The largest systematic uncertainties arise from the DeepJet correction factors and JES. The largest uncertainty sources related to background modeling and simulation are the additional jets and b jets in $\mathrm{t\bar{t}W}$ production, the impact of the $\mathrm{t\bar{t}Z}$ normalization, and the modeling of the $\mathrm{t\bar{t}t\bar{t}}$ signal process. The values of the nuisance parameters associated with additional jets or b jets in $\mathrm{t\bar{t}X}$ production after the fit are close to zero. The 20 leading nuisance parameters in the fit are shown in Fig. 9.

Table 2: Number of predicted and observed events in the SR-2ℓ and SR-3ℓ $t\bar{t}t\bar{t}$ classes, both before the fit to the data ("prefit") and with their best fit normalizations ("postfit"). The uncertainties in the predicted number of events include both the statistical and systematic components. The uncertainties in the total number of predicted background and background plus signal events are also given. A dash indicates that the corresponding background does not contribute.

Process	SR-2ℓ $t\bar{t}t\bar{t}$ class		SR-3ℓ $t\bar{t}t\bar{t}$ class	
	Prefit	Postfit	Prefit	Postfit
$t\bar{t}t\bar{t}$	35.85 ± 0.36	46.5 ± 1.8	16.92 ± 0.26	22.4 ± 1.5
ttt	3.05 ± 0.10	2.98 ± 0.13	1.44 ± 0.08	1.45 ± 0.11
$t\bar{t}W$	40.8 ± 2.0	52.7 ± 2.1	14.5 ± 1.2	19.6 ± 1.6
$t\bar{t}Z$	14.31 ± 0.45	15.95 ± 0.56	22.6 ± 1.0	26.3 ± 1.0
$t\bar{t}H$	24.28 ± 0.97	23.29 ± 0.95	21.0 ± 1.2	21.0 ± 1.2
Other t	7.06 ± 0.26	6.86 ± 0.29	4.70 ± 0.36	4.81 ± 0.36
WZ	1.27 ± 0.50	1.19 ± 0.52	2.67 ± 0.83	3.41 ± 1.13
VV(V)	0.38 ± 0.09	0.35 ± 0.06	0.26 ± 0.13	0.20 ± 0.09
$X\gamma$	15.0 ± 1.1	14.0 ± 1.0	6.87 ± 0.57	7.1 ± 1.0
Charge misID	8.24 ± 0.21	8.29 ± 0.21	—	—
Nonprompt e	32.1 ± 2.5	37.8 ± 1.1	13.3 ± 2.0	16.40 ± 0.97
Nonprompt μ	10.7 ± 2.1	12.60 ± 0.67	4.8 ± 1.3	5.87 ± 0.61
Total background	157.2 ± 4.1	175.9 ± 3.0	92.0 ± 3.2	106.1 ± 2.9
Total prediction	193.1 ± 4.2	222.5 ± 3.5	108.9 ± 3.3	128.5 ± 3.3
Data	232		135	

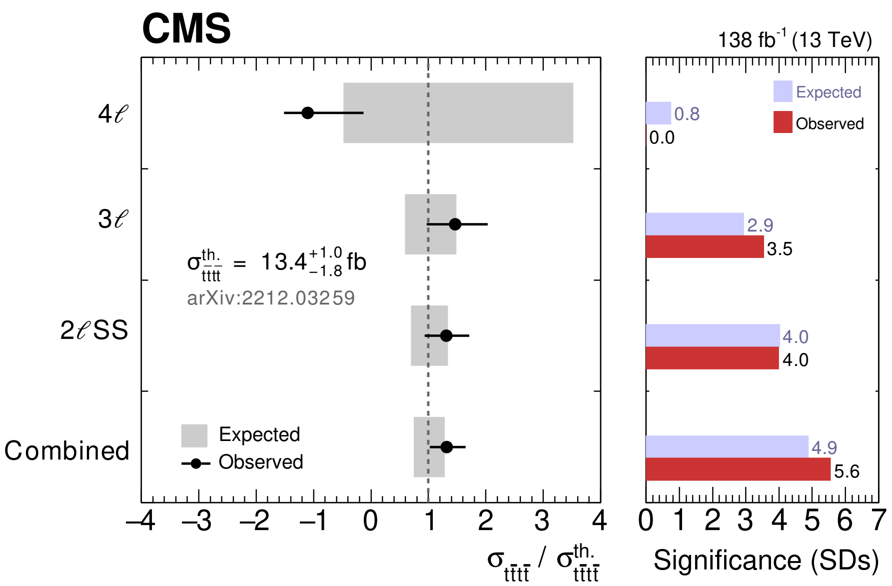

Figure 8: Comparison of fit results in the channels individually and in their combination. The left panel shows the values of the measured cross section relative to the SM prediction from Ref. [6], where the displayed uncertainty does not include the uncertainty in the SM prediction. The right panel shows the expected and observed significance, with the printed values rounded to the first decimal.

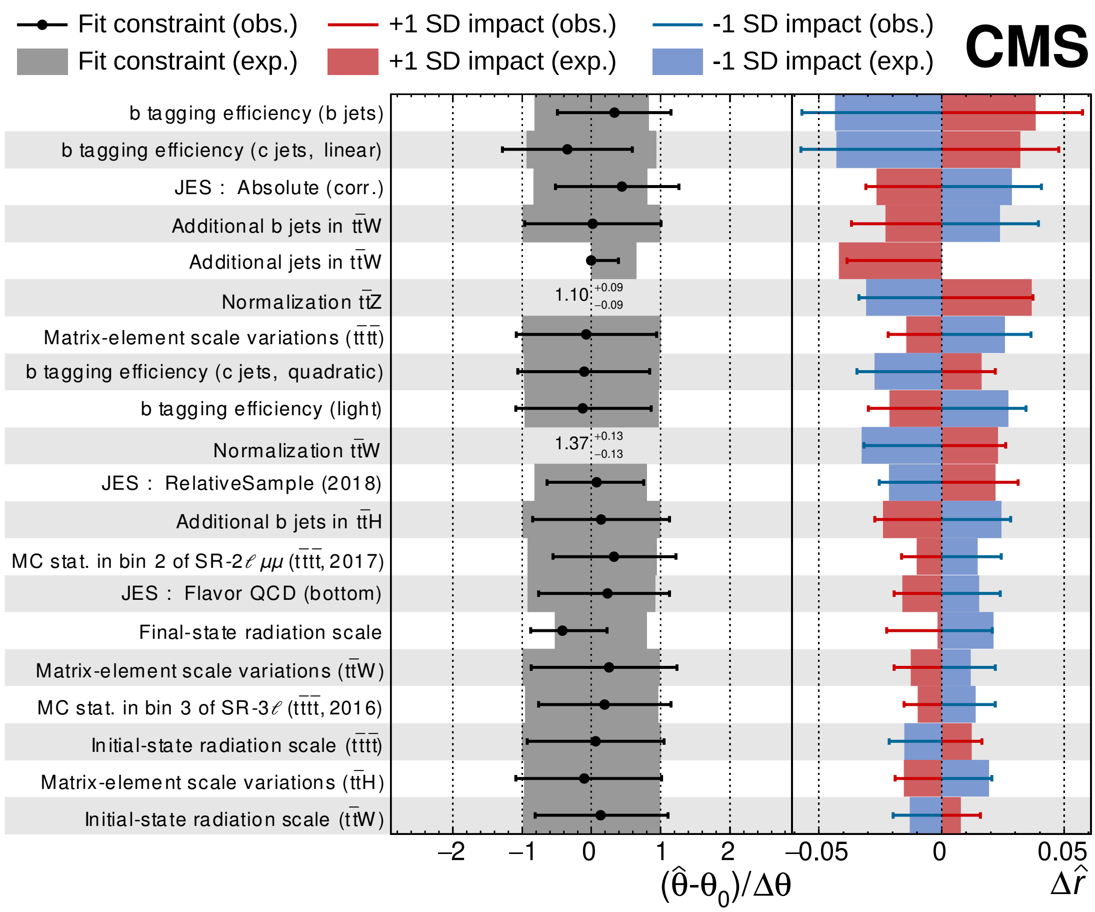

Figure 9: For the nuisance parameters listed in the left column, the pulls $(\widehat{\theta} - \theta_0)/\Delta\theta$ (middle column) and impacts $\Delta\widehat{r}$ (right column) are displayed. The 20 nuisance parameters with the largest impacts in the fit used to determine the $\mathrm{t\bar{t}t\bar{t}}$ cross section are shown. The impact $\Delta\widehat{r}$ is obtained from varying the nuisance parameter θ by ± 1 SD and evaluating the induced shift in the $\mathrm{t\bar{t}t\bar{t}}$ signal strength r. The pull $(\widehat{\theta} - \theta_0)/\Delta\theta$ is calculated from the values $\widehat{\theta}$ and θ_0 after and before the fit of θ, respectively, and from its uncertainty $\Delta\theta$ before the fit. The label "corr." and the per-year labels indicate nuisance parameters associated with the correlated and uncorrelated parts of a systematic uncertainty, respectively. The nuisance parameters labeled "MC stat." refer to the per-bin statistical uncertainties in the predicted yields. The uncertainty associated with additional jets in $\mathrm{t\bar{t}W}$ production corresponds to a one-sided variation of the nominal template before the fit, and thus a one-sided impact after the fit is expected.

The cross sections of the $\mathrm{t\bar{t}W}$ and $\mathrm{t\bar{t}Z}$ backgrounds are found to be

$$\sigma(\mathrm{t\bar{t}W}) = 990 \pm 58\,(\mathrm{stat}) \pm 79\,(\mathrm{syst})\,\mathrm{fb} = 990 \pm 98\,\mathrm{fb},$$
$$\sigma(\mathrm{t\bar{t}Z}) = 945 \pm 43\,(\mathrm{stat}) \pm 69\,(\mathrm{syst})\,\mathrm{fb} = 945 \pm 81\,\mathrm{fb}.$$

The $\mathrm{t\bar{t}W}$ cross section result is larger than the SM prediction of 722 ± 74 fb [98] at the level of 2.2 SDs, and also larger by more than 1.0 SDs than the central value $868 \pm 40\,(\mathrm{stat}) \pm 51\,(\mathrm{syst})$ fb from the dedicated CMS cross section measurement based on the same data set using same-sign 2ℓ and 3ℓ events [119]. The measured $\mathrm{t\bar{t}Z}$ cross section is in agreement with the SM prediction of 859 ± 80 fb [99] at the level of 0.8 SDs, and also in good agreement with the dedicated CMS cross section measurement of $950 \pm 50\,(\mathrm{stat}) \pm 60\,(\mathrm{syst})$ fb based on a partial data set of $77.5\,\mathrm{fb}^{-1}$ using 3ℓ and 4ℓ events [102].

9 Summary

A measurement of the production of four top quarks ($\mathrm{t\bar{t}t\bar{t}}$) in proton-proton collisions at $\sqrt{s} =$ 13 TeV has been presented, using events with two same-sign, three, and four charged leptons (electrons and muons) and additional jets from a data set corresponding to an integrated luminosity of 138 $\mathrm{fb^{-1}}$ recorded with the CMS detector at the LHC. Multivariate discriminants are employed in the identification of prompt leptons and jets originating from the decay of b hadrons, and to distinguish between selected events from the $\mathrm{t\bar{t}t\bar{t}}$ signal and the main background contributions. A profile likelihood fit is performed to the data in signal and control regions for the extraction of the $\mathrm{t\bar{t}t\bar{t}}$ cross section.

The improvements in object identification and analysis strategy bring the sensitivity of the analysis to the observation level, with an observed (expected) significance of the $\mathrm{t\bar{t}t\bar{t}}$ signal above the background-only hypothesis of 5.6 (4.9) standard deviations. The signal cross section is measured to be $\sigma(\mathrm{t\bar{t}t\bar{t}}) = 17.7\,^{+3.7}_{-3.5}\,(\mathrm{stat})\,^{+2.3}_{-1.9}\,(\mathrm{syst})\,\mathrm{fb}$, in agreement with the available standard model predictions. This result marks a significant milestone in the top quark physics program of the LHC.

Acknowledgments

We congratulate our colleagues in the CERN accelerator departments for the excellent performance of the LHC and thank the technical and administrative staffs at CERN and at other CMS institutes for their contributions to the success of the CMS effort. In addition, we gratefully acknowledge the computing centres and personnel of the Worldwide LHC Computing Grid and other centres for delivering so effectively the computing infrastructure essential to our analyses. Finally, we acknowledge the enduring support for the construction and operation of the LHC, the CMS detector, and the supporting computing infrastructure provided by the following funding agencies: BMBWF and FWF (Austria); FNRS and FWO (Belgium); CNPq, CAPES, FAPERJ, FAPERGS, and FAPESP (Brazil); MES and BNSF (Bulgaria); CERN; CAS, MoST, and NSFC (China); MINCIENCIAS (Colombia); MSES and CSF (Croatia); RIF (Cyprus); SENESCYT (Ecuador); MoER, ERC PUT and ERDF (Estonia); Academy of Finland, MEC, and HIP (Finland); CEA and CNRS/IN2P3 (France); BMBF, DFG, and HGF (Germany); GSRI (Greece); NKFIH (Hungary); DAE and DST (India); IPM (Iran); SFI (Ireland); INFN (Italy); MSIP and NRF (Republic of Korea); MES (Latvia); LAS (Lithuania); MOE and UM (Malaysia); BUAP, CINVESTAV, CONACYT, LNS, SEP, and UASLP-FAI (Mexico); MOS (Montenegro); MBIE (New Zealand); PAEC (Pakistan); MES and NSC (Poland); FCT (Portugal); MESTD (Serbia); MCIN/AEI and PCTI (Spain); MOSTR (Sri Lanka); Swiss Funding Agencies (Switzerland); MST (Taipei); MHESI and NSTDA (Thailand); TUBITAK and TENMAK (Turkey); NASU (Ukraine); STFC (United Kingdom); DOE and NSF (USA).

Individuals have received support from the Marie-Curie programme and the European Research Council and Horizon 2020 Grant, contract Nos. 675440, 724704, 752730, 758316, 765710, 824093, 884104, and COST Action CA16108 (European Union); the Leventis Foundation; the Alfred P. Sloan Foundation; the Alexander von Humboldt Foundation; the Belgian Federal Science Policy Office; the Fonds pour la Formation à la Recherche dans l'Industrie et dans l'Agriculture (FRIA-Belgium); the Agentschap voor Innovatie door Wetenschap en Technologie (IWT-Belgium); the F.R.S.-FNRS and FWO (Belgium) under the "Excellence of Science – EOS" – be.h project n. 30820817; the Beijing Municipal Science & Technology Commission, No. Z191100007219010; the Ministry of Education, Youth and Sports (MEYS) of the Czech Republic; the Hellenic Foundation for Research and Innovation (HFRI), Project Number 2288

(Greece); the Deutsche Forschungsgemeinschaft (DFG), under Germany's Excellence Strategy – EXC 2121 "Quantum Universe" – 390833306, and under project number 400140256 - GRK2497; the Hungarian Academy of Sciences, the New National Excellence Program - ÚNKP, the NKFIH research grants K 124845, K 124850, K 128713, K 128786, K 129058, K 131991, K 133046, K 138136, K 143460, K 143477, 2020-2.2.1-ED-2021-00181, and TKP2021-NKTA-64 (Hungary); the Council of Science and Industrial Research, India; the Latvian Council of Science; the Ministry of Education and Science, project no. 2022/WK/14, and the National Science Center, contracts Opus 2021/41/B/ST2/01369 and 2021/43/B/ST2/01552 (Poland); the Fundação para a Ciência e a Tecnologia, grant CEECIND/01334/2018 (Portugal); the National Priorities Research Program by Qatar National Research Fund; MCIN/AEI/10.13039/501100011033, ERDF "a way of making Europe", and the Programa Estatal de Fomento de la Investigación Científica y Técnica de Excelencia María de Maeztu, grant MDM-2017-0765 and Programa Severo Ochoa del Principado de Asturias (Spain); the Chulalongkorn Academic into Its 2nd Century Project Advancement Project, and the National Science, Research and Innovation Fund via the Program Management Unit for Human Resources & Institutional Development, Research and Innovation, grant B05F650021 (Thailand); the Kavli Foundation; the Nvidia Corporation; the SuperMicro Corporation; the Welch Foundation, contract C-1845; and the Weston Havens Foundation (USA).

References

[1] G. Bevilacqua and M. Worek, "Constraining BSM physics at the LHC: Four top final states with NLO accuracy in perturbative QCD", *JHEP* **07** (2012) 111, doi:10.1007/JHEP07(2012)111, arXiv:1206.3064.

[2] J. Alwall et al., "The automated computation of tree-level and next-to-leading order differential cross sections, and their matching to parton shower simulations", *JHEP* **07** (2014) 079, doi:10.1007/JHEP07(2014)079, arXiv:1405.0301.

[3] F. Maltoni, D. Pagani, and I. Tsinikos, "Associated production of a top-quark pair with vector bosons at NLO in QCD: impact on $\mathrm{t\bar{t}H}$ searches at the LHC", *JHEP* **02** (2016) 113, doi:10.1007/JHEP02(2016)113, arXiv:1507.05640.

[4] R. Frederix, D. Pagani, and M. Zaro, "Large NLO corrections in $\mathrm{t\bar{t}W^{\pm}}$ and $\mathrm{t\bar{t}t\bar{t}}$ hadroproduction from supposedly subleading EW contributions", *JHEP* **02** (2018) 031, doi:10.1007/JHEP02(2018)031, arXiv:1711.02116.

[5] T. Ježo and M. Kraus, "Hadroproduction of four top quarks in the POWHEG BOX", *Phys. Rev. D* **105** (2022) 114024, doi:10.1103/PhysRevD.105.114024, arXiv:2110.15159.

[6] M. van Beekveld, A. Kulesza, and L. Moreno Valero, "Threshold resummation for the production of four top quarks at the LHC", 2022. arXiv:2212.03259.

[7] Q.-H. Cao, S.-L. Chen, and Y. Liu, "Probing Higgs width and top quark Yukawa coupling from $\mathrm{t\bar{t}H}$ and $\mathrm{t\bar{t}t\bar{t}}$ productions", *Phys. Rev. D* **95** (2017) 053004, doi:10.1103/PhysRevD.95.053004, arXiv:1602.01934.

[8] Q.-H. Cao et al., "Limiting top quark-Higgs boson interaction and Higgs-boson width from multitop productions", *Phys. Rev. D* **99** (2019) 113003, doi:10.1103/PhysRevD.99.113003, arXiv:1901.04567.

[9] CMS Collaboration, "Measurement of the Higgs boson production rate in association with top quarks in final states with electrons, muons, and hadronically decaying tau leptons at $\sqrt{s} = 13\,\mathrm{TeV}$", *Eur. Phys. J. C* **81** (2021) 378, doi:10.1140/epjc/s10052-021-09014-x, arXiv:2011.03652.

[10] CMS Collaboration, "Measurement of the top quark Yukawa coupling from $\mathrm{t\bar{t}}$ kinematic distributions in the lepton+jets final state in proton-proton collisions at $\sqrt{s} = 13\,\mathrm{TeV}$", *Phys. Rev. D* **100** (2019) 072007, doi:10.1103/PhysRevD.100.072007, arXiv:1907.01590.

[11] CMS Collaboration, "Measurement of the top quark Yukawa coupling from $\mathrm{t\bar{t}}$ kinematic distributions in the dilepton final state in proton-proton collisions at $\sqrt{s} = 13\,\mathrm{TeV}$", *Phys. Rev. D* **102** (2020) 092013, doi:10.1103/PhysRevD.102.092013, arXiv:2009.07123.

[12] D. Dicus, A. Stange, and S. Willenbrock, "Higgs decay to top quarks at hadron colliders", *Phys. Lett. B* **333** (1994) 126, doi:10.1016/0370-2693(94)91017-0, arXiv:hep-ph/9404359.

[13] N. Craig et al., "The hunt for the rest of the Higgs bosons", *JHEP* **06** (2015) 137, doi:10.1007/JHEP06(2015)137, arXiv:1504.04630.

[14] N. Craig et al., "Heavy Higgs bosons at low tan β: from the LHC to 100 TeV", *JHEP* **01** (2017) 018, doi:10.1007/JHEP01(2017)018, arXiv:1605.08744.

[15] Anisha et al., "On the BSM reach of four top production at the LHC", 2023. arXiv:2302.08281. Submitted to *JHEP*.

[16] H. Nilles, "Supersymmetry, supergravity and particle physics", *Phys. Rept.* **110** (1984) 1, doi:10.1016/0370-1573(84)90008-5.

[17] G. Farrar and P. Fayet, "Phenomenology of the production, decay, and detection of new hadronic states associated with supersymmetry", *Phys. Lett. B* **76** (1978) 575, doi:10.1016/0370-2693(78)90858-4.

[18] M. Toharia and J. Wells, "Gluino decays with heavier scalar superpartners", *JHEP* **02** (2006) 015, doi:10.1088/1126-6708/2006/02/015, arXiv:hep-ph/0503175.

[19] T. Plehn and T. Tait, "Seeking sgluons", *J. Phys. G* **36** (2009) 075001, doi:10.1088/0954-3899/36/7/075001, arXiv:0810.3919.

[20] S. Calvet, B. Fuks, P. Gris, and L. Valery, "Searching for sgluons in multitop events at a center-of-mass energy of 8 TeV", *JHEP* **04** (2013) 043, doi:10.1007/JHEP04(2013)043, arXiv:1212.3360.

[21] L. Beck et al., "Probing top-philic sgluons with LHC Run I data", *Phys. Lett. B* **746** (2015) 48, doi:10.1016/j.physletb.2015.04.043, arXiv:1501.07580.

[22] L. Darmé, B. Fuks, and M. Goodsell, "Cornering sgluons with four-top-quark events", *Phys. Lett. B* **784** (2018) 223, doi:10.1016/j.physletb.2018.08.001, arXiv:1805.10835.

[23] K. Kumar, T. M. P. Tait, and R. Vega-Morales, "Manifestations of top compositeness at colliders", *JHEP* **05** (2009) 022, doi:10.1088/1126-6708/2009/05/022, arXiv:0901.3808.

[24] G. Cacciapaglia et al., "Composite scalars at the LHC: the Higgs, the sextet and the octet", *JHEP* **11** (2015) 201, doi:10.1007/JHEP11(2015)201, arXiv:1507.02283.

[25] O. Ducu, L. Heurtier, and J. Maurer, "LHC signatures of a Z' mediator between dark matter and the SU(3) sector", *JHEP* **03** (2016) 006, doi:10.1007/JHEP03(2016)006, arXiv:1509.05615.

[26] C. Degrande et al., "Non-resonant new physics in top pair production at hadron colliders", *JHEP* **03** (2011) 125, doi:10.1007/JHEP03(2011)125, arXiv:1010.6304.

[27] C. Zhang, "Constraining qqtt operators from four-top production: a case for enhanced EFT sensitivity", *Chin. Phys. C* **42** (2018) 023104, doi:10.1088/1674-1137/42/2/023104, arXiv:1708.05928.

[28] N. Hartland et al., "A Monte Carlo global analysis of the standard model effective field theory: the top quark sector", *JHEP* **04** (2019) 100, doi:10.1007/JHEP04(2019)100, arXiv:1901.05965.

[29] C. Englert, G. F. Giudice, A. Greljo, and M. McCullough, "The $\widehat{\mathrm{H}}$-parameter: an oblique Higgs view", *JHEP* **09** (2019) 041, doi:10.1007/JHEP09(2019)041, arXiv:1903.07725.

[30] G. Banelli et al., "The present and future of four top operators", *JHEP* **02** (2021) 043, doi:10.1007/JHEP02(2021)043, arXiv:2010.05915.

[31] L. Darmé, B. Fuks, and F. Maltoni, "Top-philic heavy resonances in four-top final states and their EFT interpretation", *JHEP* **09** (2021) 143, doi:10.1007/JHEP09(2021)143, arXiv:2104.09512.

[32] SMEFiT Collaboration, "Combined SMEFT interpretation of Higgs, diboson, and top quark data from the LHC", *JHEP* **11** (2021) 089, doi:10.1007/JHEP11(2021)089, arXiv:2105.00006.

[33] R. Aoude, H. El Faham, F. Maltoni, and E. Vryonidou, "Complete SMEFT predictions for four top quark production at hadron colliders", *JHEP* **10** (2022) 163, doi:10.1007/JHEP10(2022)163, arXiv:2208.04962.

[34] ATLAS Collaboration, "The ATLAS experiment at the CERN Large Hadron Collider", *JINST* **3** (2008) S08003, doi:10.1088/1748-0221/3/08/S08003.

[35] CMS Collaboration, "The CMS experiment at the CERN LHC", *JINST* **3** (2008) S08004, doi:10.1088/1748-0221/3/08/S08004.

[36] CMS Collaboration, "Search for physics beyond the standard model in events with two leptons of same sign, missing transverse momentum, and jets in proton-proton collisions at $\sqrt{s} = 13\,\text{TeV}$", *Eur. Phys. J. C* **77** (2017) 578, doi:10.1140/epjc/s10052-017-5079-z, arXiv:1704.07323.

[37] CMS Collaboration, "Search for standard model production of four top quarks with same-sign and multilepton final states in proton-proton collisions at $\sqrt{s} = 13\,\text{TeV}$", *Eur. Phys. J. C* **78** (2018) 140, doi:10.1140/epjc/s10052-018-5607-5, arXiv:1710.10614.

[38] ATLAS Collaboration, "Search for new phenomena in events with same-charge leptons and b jets in pp collisions at $\sqrt{s} = 13\,\text{TeV}$ with the ATLAS detector", *JHEP* **12** (2018) 039, doi:10.1007/JHEP12(2018)039, arXiv:1807.11883.

[39] ATLAS Collaboration, "Search for four-top-quark production in the single-lepton and opposite-sign dilepton final states in pp collisions at $\sqrt{s} = 13\,\text{TeV}$ with the ATLAS detector", *Phys. Rev. D* **99** (2019) 052009, doi:10.1103/PhysRevD.99.052009, arXiv:1811.02305.

[40] CMS Collaboration, "Search for the production of four top quarks in the single-lepton and opposite-sign dilepton final states in proton-proton collisions at $\sqrt{s} = 13\,\text{TeV}$", *JHEP* **11** (2019) 082, doi:10.1007/JHEP11(2019)082, arXiv:1906.02805.

[41] CMS Collaboration, "Search for production of four top quarks in final states with same-sign or multiple leptons in proton-proton collisions at $\sqrt{s} = 13\,\text{TeV}$", *Eur. Phys. J. C* **80** (2020) 75, doi:10.1140/epjc/s10052-019-7593-7, arXiv:1908.06463.

[42] ATLAS Collaboration, "Evidence for $\mathrm{t\bar{t}t\bar{t}}$ production in the multilepton final state in proton-proton collisions at $\sqrt{s} = 13\,\text{TeV}$ with the ATLAS detector", *Eur. Phys. J. C* **80** (2020) 1085, doi:10.1140/epjc/s10052-020-08509-3, arXiv:2007.14858.

[43] ATLAS Collaboration, "Measurement of the $\mathrm{t\bar{t}t\bar{t}}$ production cross section in pp collisions at $\sqrt{s} = 13\,\text{TeV}$ with the ATLAS detector", *JHEP* **11** (2021) 118, doi:10.1007/JHEP11(2021)118, arXiv:2106.11683.

[44] CMS Collaboration, "Evidence for four-top quark production in proton-proton collisions at $\sqrt{s} = 13$ TeV", 2023. arXiv:2303.03864. Submitted to *Phys. Lett. B*.

[45] F. Blekman, F. Déliot, V. Dutta, and E. Usai, "Four-top quark physics at the LHC", *Universe* **8** (2022) 638, doi:10.3390/universe8120638, arXiv:2208.04085.

[46] L. Lyons and N. Wardle, "Statistical issues in searches for new phenomena in high energy physics", *J. Phys. G* **45** (2018) 033001, doi:10.1088/1361-6471/aa9408.

[47] ATLAS Collaboration, "Observation of four-top-quark production in the multilepton final state with the ATLAS detector", 2023. arXiv:2303.15061. Submitted to *Eur. Phys. J. C*.

[48] HEPData record for this analysis, 2023. doi:10.17182/hepdata.138420.

[49] CMS Collaboration, "Performance of the CMS Level-1 trigger in proton-proton collisions at $\sqrt{s} = 13$ TeV", *JINST* **15** (2020) P10017, doi:10.1088/1748-0221/15/10/P10017, arXiv:2006.10165.

[50] CMS Collaboration, "The CMS trigger system", *JINST* **12** (2017) P01020, doi:10.1088/1748-0221/12/01/P01020, arXiv:1609.02366.

[51] CMS Collaboration, "Particle-flow reconstruction and global event description with the CMS detector", *JINST* **12** (2017) P10003, doi:10.1088/1748-0221/12/10/P10003, arXiv:1706.04965.

[52] CMS Collaboration, "Technical proposal for the Phase-II upgrade of the Compact Muon Solenoid", CMS Technical Proposal CERN-LHCC-2015-010, CMS-TDR-15-02, 2015.

[53] M. Cacciari, G. P. Salam, and G. Soyez, "The anti-k_{T} jet clustering algorithm", *JHEP* **04** (2008) 063, doi:10.1088/1126-6708/2008/04/063, arXiv:0802.1189.

[54] M. Cacciari, G. P. Salam, and G. Soyez, "FastJet user manual", *Eur. Phys. J. C* **72** (2012) 1896, doi:10.1140/epjc/s10052-012-1896-2, arXiv:1111.6097.

[55] CMS Collaboration, "Jet energy scale and resolution in the CMS experiment in pp collisions at 8 TeV", *JINST* **12** (2017) P02014, doi:10.1088/1748-0221/12/02/P02014, arXiv:1607.03663.

[56] CMS Collaboration, "Performance of missing transverse momentum reconstruction in proton-proton collisions at $\sqrt{s} = 13$ TeV using the CMS detector", *JINST* **14** (2019) P07004, doi:10.1088/1748-0221/14/07/P07004, arXiv:1903.06078.

[57] CMS Collaboration, "Identification of heavy-flavour jets with the CMS detector in pp collisions at 13 TeV", *JINST* **13** (2018) P05011, doi:10.1088/1748-0221/13/05/P05011, arXiv:1712.07158.

[58] E. Bols et al., "Jet flavour classification using DeepJet", *JINST* **15** (2020) P12012, doi:10.1088/1748-0221/15/12/P12012, arXiv:2008.10519.

[59] CMS Collaboration, "Performance summary of AK4 jet b tagging with data from proton-proton collisions at 13 TeV with the CMS detector", CMS Detector Performance Note CMS-DP-2023-005, 2023.

[60] P. Artoisenet, R. Frederix, O. Mattelaer, and R. Rietkerk, "Automatic spin-entangled decays of heavy resonances in Monte Carlo simulations", *JHEP* **03** (2013) 015, doi:10.1007/JHEP03(2013)015, arXiv:1212.3460.

[61] P. Nason, "A new method for combining NLO QCD with shower Monte Carlo algorithms", *JHEP* **11** (2004) 040, doi:10.1088/1126-6708/2004/11/040, arXiv:hep-ph/0409146.

[62] S. Frixione, G. Ridolfi, and P. Nason, "A positive-weight next-to-leading-order Monte Carlo for heavy flavour hadroproduction", *JHEP* **09** (2007) 126, doi:10.1088/1126-6708/2007/09/126, arXiv:0707.3088.

[63] S. Frixione, P. Nason, and C. Oleari, "Matching NLO QCD computations with parton shower simulations: the POWHEG method", *JHEP* **11** (2007) 070, doi:10.1088/1126-6708/2007/11/070, arXiv:0709.2092.

[64] S. Alioli, P. Nason, C. Oleari, and E. Re, "NLO single-top production matched with shower in POWHEG: *s*- and *t*-channel contributions", *JHEP* **09** (2009) 111, doi:10.1088/1126-6708/2009/09/111, arXiv:0907.4076. [Erratum: doi:10.1007/JHEP02(2010)011].

[65] P. Nason and C. Oleari, "NLO Higgs boson production via vector-boson fusion matched with shower in POWHEG", *JHEP* **02** (2010) 037, doi:10.1007/JHEP02(2010)037, arXiv:0911.5299.

[66] S. Alioli, P. Nason, C. Oleari, and E. Re, "A general framework for implementing NLO calculations in shower Monte Carlo programs: the POWHEG BOX", *JHEP* **06** (2010) 043, doi:10.1007/JHEP06(2010)043, arXiv:1002.2581.

[67] E. Re, "Single-top W*t*-channel production matched with parton showers using the POWHEG method", *Eur. Phys. J. C* **71** (2011) 1547, doi:10.1140/epjc/s10052-011-1547-z, arXiv:1009.2450.

[68] E. Bagnaschi, G. Degrassi, P. Slavich, and A. Vicini, "Higgs production via gluon fusion in the POWHEG approach in the SM and in the MSSM", *JHEP* **02** (2012) 088, doi:10.1007/JHEP02(2012)088, arXiv:1111.2854.

[69] P. Nason and G. Zanderighi, "W^+W^-, WZ and ZZ production in the POWHEG-BOX-V2", *Eur. Phys. J. C* **74** (2014) 2702, doi:10.1140/epjc/s10052-013-2702-5, arXiv:1311.1365.

[70] J. M. Campbell and R. K. Ellis, "An update on vector boson pair production at hadron colliders", *Phys. Rev. D* **60** (1999) 113006, doi:10.1103/PhysRevD.60.113006, arXiv:hep-ph/9905386.

[71] J. M. Campbell, R. K. Ellis, and C. Williams, "Vector boson pair production at the LHC", *JHEP* **07** (2011) 018, doi:10.1007/JHEP07(2011)018, arXiv:1105.0020.

[72] J. M. Campbell, R. K. Ellis, and W. T. Giele, "A multi-threaded version of MCFM", *Eur. Phys. J. C* **75** (2015) 246, doi:10.1140/epjc/s10052-015-3461-2, arXiv:1503.06182.

[73] NNPDF Collaboration, "Parton distributions from high-precision collider data", *Eur. Phys. J. C* **77** (2017) 663, doi:10.1140/epjc/s10052-017-5199-5, arXiv:1706.00428.

[74] T. Sjöstrand et al., "An introduction to PYTHIA 8.2", *Comput. Phys. Commun.* **191** (2015) 159, doi:10.1016/j.cpc.2015.01.024, arXiv:1410.3012.

[75] CMS Collaboration, "Extraction and validation of a new set of CMS PYTHIA 8 tunes from underlying-event measurements", *Eur. Phys. J. C* **80** (2020) 4, doi:10.1140/epjc/s10052-019-7499-4, arXiv:1903.12179.

[76] R. Frederix and S. Frixione, "Merging meets matching in MC@NLO", *JHEP* **12** (2012) 061, doi:10.1007/JHEP12(2012)061, arXiv:1209.6215.

[77] J. Alwall et al., "Comparative study of various algorithms for the merging of parton showers and matrix elements in hadronic collisions", *Eur. Phys. J. C* **53** (2008) 473, doi:10.1140/epjc/s10052-007-0490-5, arXiv:0706.2569.

[78] S. Bolognesi et al., "On the spin and parity of a single-produced resonance at the LHC", *Phys. Rev. D* **86** (2012) 095031, doi:10.1103/PhysRevD.86.095031, arXiv:1208.4018.

[79] GEANT4 Collaboration, "GEANT4—a simulation toolkit", *Nucl. Instrum. Meth. A* **506** (2003) 250, doi:10.1016/S0168-9002(03)01368-8.

[80] CMS Collaboration, "Electron and photon reconstruction and identification with the CMS experiment at the CERN LHC", *JINST* **16** (2021) P05014, doi:10.1088/1748-0221/16/05/P05014, arXiv:2012.06888.

[81] CMS Collaboration, "ECAL 2016 refined calibration and Run2 summary plots", CMS Detector Performance Note CMS-DP-2020-021, 2020.

[82] CMS Collaboration, "Performance of electron reconstruction and selection with the CMS detector in proton-proton collisions at $\sqrt{s} = 8$ TeV", *JINST* **10** (2015) P06005, doi:10.1088/1748-0221/10/06/P06005, arXiv:1502.02701.

[83] CMS Collaboration, "Performance of the CMS muon detector and muon reconstruction with proton-proton collisions at $\sqrt{s} = 13$ TeV", *JINST* **13** (2018) P06015, doi:10.1088/1748-0221/13/06/P06015, arXiv:1804.04528.

[84] CMS Collaboration, "Performance of CMS muon reconstruction in cosmic-ray events", *JINST* **5** (2010) T03022, doi:10.1088/1748-0221/5/03/T03022, arXiv:0911.4994.

[85] CMS Collaboration, "Performance of the reconstruction and identification of high-momentum muons in proton-proton collisions at $\sqrt{s} = 13$ TeV", *JINST* **15** (2020) P02027, doi:10.1088/1748-0221/15/02/P02027, arXiv:1912.03516.

[86] K. Rehermann and B. Tweedie, "Efficient identification of boosted semileptonic top quarks at the LHC", *JHEP* **03** (2011) 059, doi:10.1007/JHEP03(2011)059, arXiv:1007.2221.

[87] T. Chen and C. Guestrin, "XGBOOST: A scalable tree boosting system", in *Proc. 22nd ACM SIGKDD Int. Conf. on Knowledge Discovery and Data Mining: San Francisco CA, USA, August 13–17, 2016*. 2016. arXiv:1603.02754. doi:10.1145/2939672.2939785.

[88] CMS Collaboration, "Evidence for associated production of a Higgs boson with a top quark pair in final states with electrons, muons, and hadronically decaying τ leptons at $\sqrt{s} = 13$ TeV", *JHEP* **08** (2018) 066, doi:10.1007/JHEP08(2018)066, arXiv:1803.05485.

[89] CMS Collaboration, "Observation of single top quark production in association with a Z boson in proton-proton collisions at $\sqrt{s} = 13\,\text{TeV}$", *Phys. Rev. Lett.* **122** (2019) 132003, doi:10.1103/PhysRevLett.122.132003, arXiv:1812.05900.

[90] CMS Collaboration, "Search for electroweak production of charginos and neutralinos in proton-proton collisions at $\sqrt{s} = 13\,\text{TeV}$", *JHEP* **04** (2022) 147, doi:10.1007/JHEP04(2022)147, arXiv:2106.14246.

[91] CMS Collaboration, "Measurements of the electroweak diboson production cross sections in proton-proton collisions at $\sqrt{s} = 5.02\,\text{TeV}$ using leptonic decays", *Phys. Rev. Lett.* **127** (2021) 191801, doi:10.1103/PhysRevLett.127.191801, arXiv:2107.01137.

[92] CMS Collaboration, "Inclusive and differential cross section measurements of single top quark production in association with a Z boson in proton-proton collisions at $\sqrt{s} = 13\,\text{TeV}$", *JHEP* **02** (2022) 107, doi:10.1007/JHEP02(2022)107, arXiv:2111.02860.

[93] CMS Collaboration, "Identification of prompt and isolated muons using multivariate techniques at the CMS experiment in proton-proton collisions at $\sqrt{s} = 13\,\text{TeV}$", CMS Physics Analysis Summary CMS-PAS-MUO-22-001, 2023.

[94] Particle Data Group, R. L. Workman et al., "Review of particle physics", *Prog. Theor. Exp. Phys.* **2022** (2022) 083C01, doi:10.1093/ptep/ptac097.

[95] H. Voss, A. Höcker, J. Stelzer, and F. Tegenfeldt, "TMVA, the toolkit for multivariate data analysis with ROOT", in *Proc. 11th Int. Workshop on Advanced Computing and Analysis Techniques in Phys. Research (ACAT 2017): Amsterdam, The Netherlands, April 23–27, 2007*. 2007. arXiv:physics/0703039. [PoS (ACAT2007) 040]. doi:10.22323/1.050.0040.

[96] C. G. Lester and D. J. Summers, "Measuring masses of semiinvisibly decaying particles pair produced at hadron colliders", *Phys. Lett. B* **463** (1999) 99, doi:10.1016/S0370-2693(99)00945-4, arXiv:hep-ph/9906349.

[97] C. G. Lester, "The stransverse mass, m_{T2}, in special cases", *JHEP* **05** (2011) 076, doi:10.1007/JHEP05(2011)076, arXiv:1103.5682.

[98] R. Frederix and I. Tsinikos, "On improving NLO merging for $\mathrm{t\bar{t}W}$ production", *JHEP* **11** (2021) 029, doi:10.1007/JHEP11(2021)029, arXiv:2108.07826.

[99] A. Kulesza et al., "Associated top quark pair production with a heavy boson: differential cross sections at NLO+NNLL accuracy", *Eur. Phys. J. C* **80** (2020) 428, doi:10.1140/epjc/s10052-020-7987-6, arXiv:2001.03031.

[100] G. Durieux, "Triple top-quark production at NLO in QCD". Zenodo, 2023. doi:10.5281/zenodo.7679328.

[101] CMS Collaboration, "Measurement of the associated production of a single top quark and a Z boson in pp collisions at $\sqrt{s} = 13\,\text{TeV}$", *Phys. Lett. B* **779** (2018) 358, doi:10.1016/j.physletb.2018.02.025, arXiv:1712.02825.

[102] CMS Collaboration, "Measurement of top quark pair production in association with a Z boson in proton-proton collisions at $\sqrt{s} = 13\,\text{TeV}$", *JHEP* **03** (2020) 056, doi:10.1007/JHEP03(2020)056, arXiv:1907.11270.

[103] CMS Collaboration, "Search for new physics in same-sign dilepton events in proton-proton collisions at $\sqrt{s} = 13\,\text{TeV}$", *Eur. Phys. J. C* **76** (2016) 439, doi:10.1140/epjc/s10052-016-4261-z, arXiv:1605.03171.

[104] CMS Collaboration, "Precision luminosity measurement in proton-proton collisions at $\sqrt{s} = 13\,\text{TeV}$ in 2015 and 2016 at CMS", *Eur. Phys. J. C* **81** (2021) 800, doi:10.1140/epjc/s10052-021-09538-2, arXiv:2104.01927.

[105] CMS Collaboration, "CMS luminosity measurement for the 2017 data-taking period at $\sqrt{s} = 13\,\text{TeV}$", CMS Physics Analysis Summary CMS-PAS-LUM-17-004, 2018.

[106] CMS Collaboration, "CMS luminosity measurement for the 2018 data-taking period at $\sqrt{s} = 13\,\text{TeV}$", CMS Physics Analysis Summary CMS-PAS-LUM-18-002, 2019.

[107] CMS Collaboration, "Measurements of inclusive W and Z cross sections in pp collisions at $\sqrt{s} = 7\,\text{TeV}$", *JHEP* **01** (2011) 080, doi:10.1007/JHEP01(2011)080, arXiv:1012.2466.

[108] CMS Collaboration, "Measurements of the $\text{pp} \to \text{WZ}$ inclusive and differential production cross section and constraints on charged anomalous triple gauge couplings at $\sqrt{s} = 13\,\text{TeV}$", *JHEP* **04** (2019) 122, doi:10.1007/JHEP04(2019)122, arXiv:1901.03428.

[109] CMS Collaboration, "Measurements of the $\text{pp} \to \text{ZZ}$ production cross section and the $\text{Z} \to 4\ell$ branching fraction, and constraints on anomalous triple gauge couplings at $\sqrt{s} = 13\,\text{TeV}$", *Eur. Phys. J. C* **78** (2018) 165, doi:10.1140/epjc/s10052-018-5567-9, arXiv:1709.08601.

[110] CMS Collaboration, "W^+W^- boson pair production in proton-proton collisions at $\sqrt{s} = 13\,\text{TeV}$", *Phys. Rev. D* **102** (2020) 092001, doi:10.1103/PhysRevD.102.092001, arXiv:2009.00119.

[111] CMS Collaboration, "Measurement of the inclusive and differential $\text{t}\bar{\text{t}}\gamma$ cross sections in the dilepton channel and effective field theory interpretation in proton-proton collisions at $\sqrt{s} = 13\,\text{TeV}$", *JHEP* **05** (2022) 091, doi:10.1007/JHEP05(2022)091, arXiv:2201.07301.

[112] M. Cacciari et al., "The $\text{t}\bar{\text{t}}$ cross-section at 1.8 and 1.96 TeV: a study of the systematics due to parton densities and scale dependence", *JHEP* **04** (2004) 068, doi:10.1088/1126-6708/2004/04/068, arXiv:hep-ph/0303085.

[113] J. Butterworth et al., "PDF4LHC recommendations for LHC Run II", *J. Phys. G* **43** (2016) 023001, doi:10.1088/0954-3899/43/2/023001, arXiv:1510.03865.

[114] CMS Collaboration, "Measurement of the cross section for $\text{t}\bar{\text{t}}$ production with additional jets and b jets in pp collisions at $\sqrt{s} = 13\,\text{TeV}$", *JHEP* **07** (2020) 125, doi:10.1007/JHEP07(2020)125, arXiv:2003.06467.

[115] ATLAS and CMS Collaborations, and LHC Higgs Combination Group, "Procedure for the LHC Higgs boson search combination in Summer 2011", Technical Report CMS-NOTE-2011-005, ATL-PHYS-PUB-2011-11, 2011.

[116] G. Cowan, K. Cranmer, E. Gross, and O. Vitells, "Asymptotic formulae for likelihood-based tests of new physics", *Eur. Phys. J. C* **71** (2011) 1554, doi:10.1140/epjc/s10052-011-1554-0, arXiv:1007.1727. [Erratum: doi:10.1140/epjc/s10052-013-2501-z].

[117] R. Barlow and C. Beeston, "Fitting using finite Monte Carlo samples", *Comput. Phys. Commun.* **77** (1993) 219, doi:10.1016/0010-4655(93)90005-W.

[118] J. S. Conway, "Incorporating nuisance parameters in likelihoods for multisource spectra", in *Proc. 2011 Workshop on Statistical Issues Related to Discovery Claims in Search Experiments and Unfolding (PHYSTAT 2011): Geneva, Switzerland, January 17–20, 2011*. 2011. arXiv:1103.0354. doi:10.5170/CERN-2011-006.115.

[119] CMS Collaboration, "Measurement of the cross section of top quark-antiquark pair production in association with a W boson in proton-proton collisions at $\sqrt{s} = 13\,\text{TeV}$", 2022. arXiv:2208.06485. Accepted by *JHEP*.

A Prefit distributions

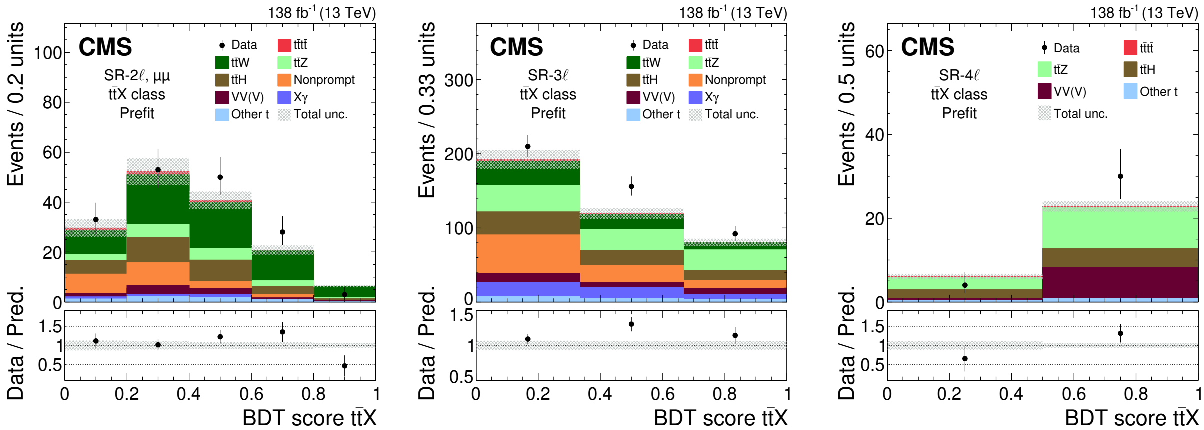

Figure A.1: Comparison of the number of observed (points) and predicted (colored histograms) events in the BDT score $t\bar{t}X$ in the $t\bar{t}X$ classes of SR-2ℓ in the $\mu\mu$ category (left), of SR-3ℓ (middle), and of SR-4ℓ (right). The vertical bars on the points represent the statistical uncertainties in the data, and the hatched bands the total uncertainty in the predictions. The signal and background yields are shown before the fit to the data ("prefit").

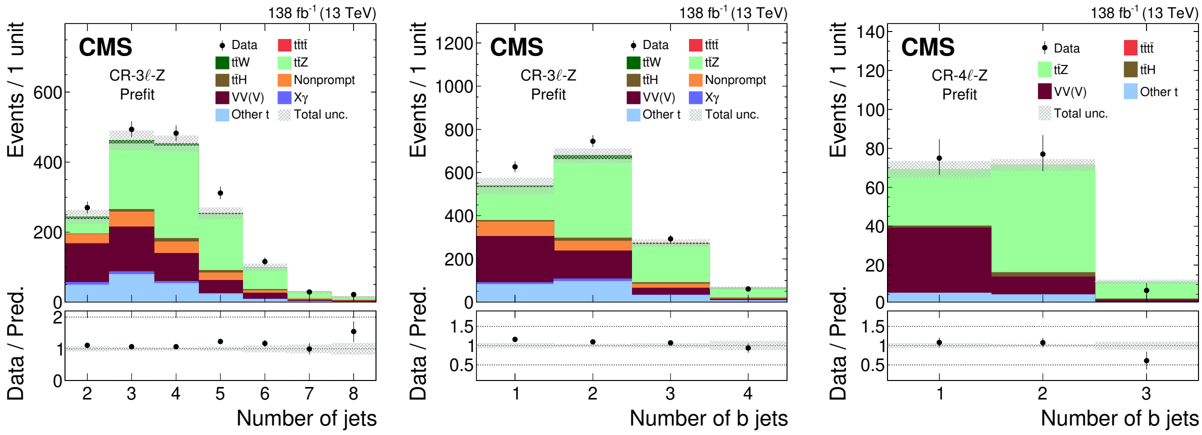

Figure A.2: Comparison of the number of observed (points) and predicted (colored histograms) events in the number of jets distribution in CR-3ℓ-Z (left), and in the number of b jets distribution in CR-3ℓ-Z (middle) and CR-4ℓ-Z (right). The vertical bars on the points represent the statistical uncertainties in the data, and the hatched bands the total uncertainty in the predictions. The signal and background yields are shown before the fit to the data ("prefit").

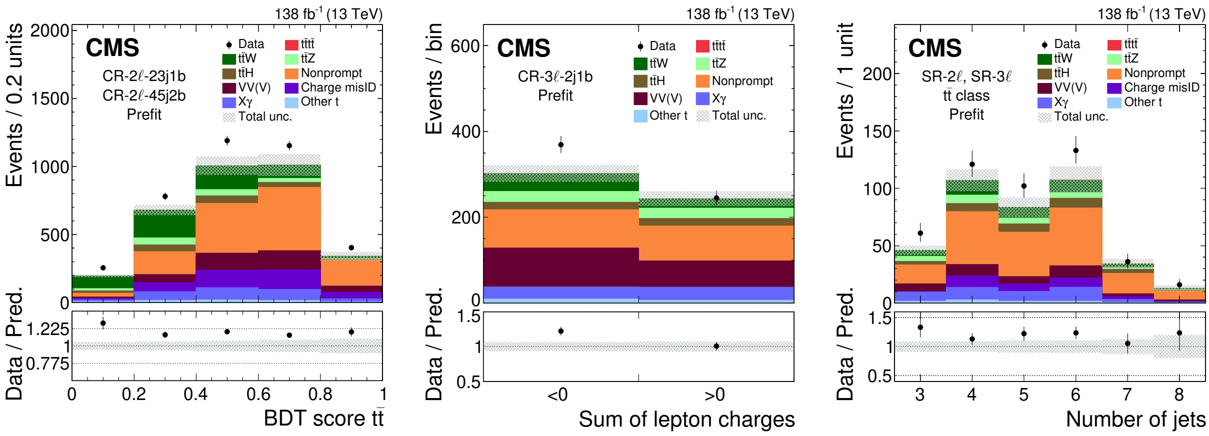

Figure A.3: Comparison of the number of observed (points) and predicted (colored histograms) events in the BDT score $t\bar{t}$ in the combined CR-2ℓ-23j1b and CR-2ℓ-45j2b (left), in the event yields with negative and positive sum of lepton charges in CR-3ℓ-2j1b (middle), and in the number of jets distribution in the $t\bar{t}$ class of the combined SR-2ℓ and SR-3ℓ (right). The vertical bars on the points represent the statistical uncertainties in the data, and the hatched bands the total uncertainty in the predictions. The signal and background yields are shown before the fit to the data ("prefit").

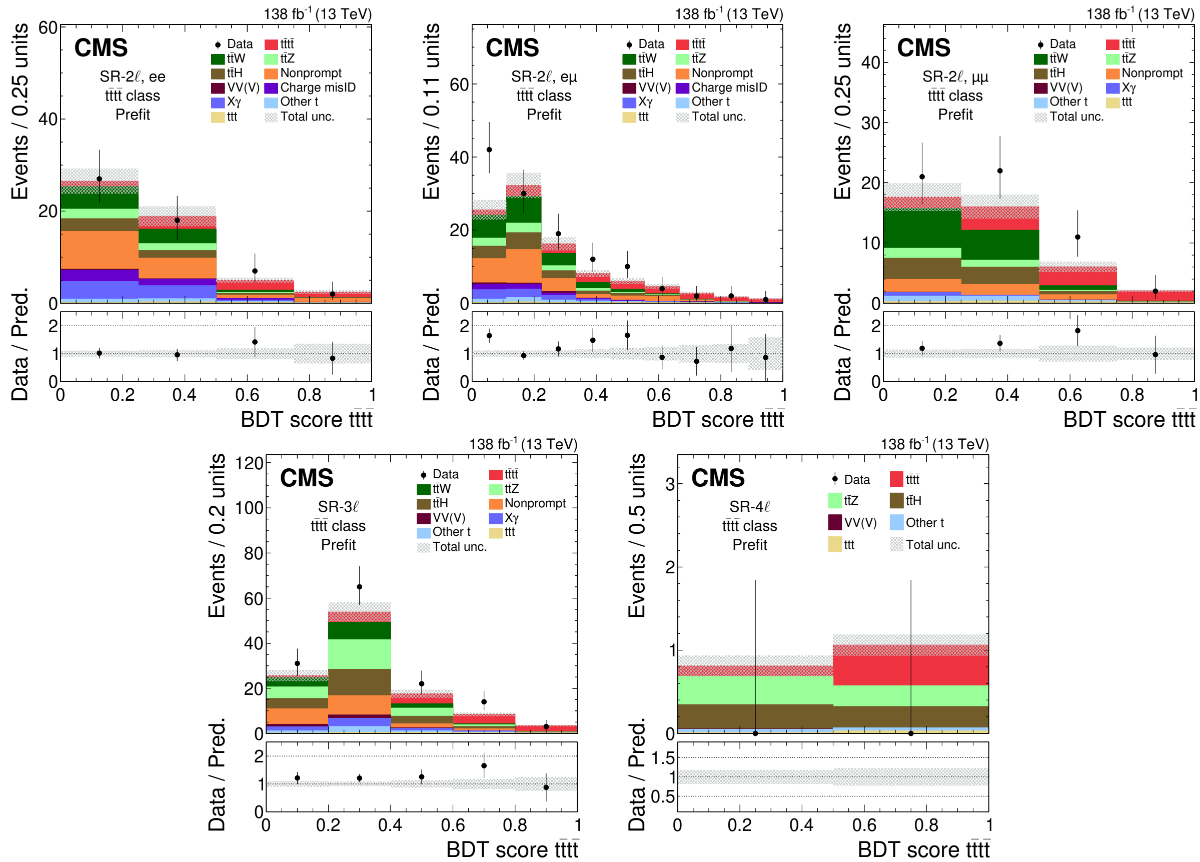

Figure A.4: Comparison of the number of observed (points) and predicted (colored histograms) events in the BDT score $t\bar{t}t\bar{t}$ in the $t\bar{t}t\bar{t}$ classes of SR-2ℓ, shown for the ee (upper left), eμ (upper middle), and $\mu\mu$ (upper right) categories, of SR-3ℓ (lower left) and of SR-4ℓ (lower right). The vertical bars on the points represent the statistical uncertainties in the data, and the hatched bands the total uncertainty in the predictions. The signal and background yields are shown before the fit to the data ("prefit").

B The CMS Collaboration

Yerevan Physics Institute, Yerevan, Armenia
A. Hayrapetyan, A. Tumasyan[1]

Institut für Hochenergiephysik, Vienna, Austria
W. Adam, J.W. Andrejkovic, T. Bergauer, S. Chatterjee, K. Damanakis, M. Dragicevic, A. Escalante Del Valle, P.S. Hussain, M. Jeitler[2], N. Krammer, D. Liko, I. Mikulec, J. Schieck[2], R. Schöfbeck, D. Schwarz, M. Sonawane, S. Templ, W. Waltenberger, C.-E. Wulz[2]

Universiteit Antwerpen, Antwerpen, Belgium
M.R. Darwish[3], T. Janssen, P. Van Mechelen

Vrije Universiteit Brussel, Brussel, Belgium
E.S. Bols, J. D'Hondt, S. Dansana, A. De Moor, M. Delcourt, H. El Faham, S. Lowette, I. Makarenko, D. Müller, A.R. Sahasransu, S. Tavernier, M. Tytgat[4], S. Van Putte, D. Vannerom

Université Libre de Bruxelles, Bruxelles, Belgium
B. Clerbaux, G. De Lentdecker, L. Favart, D. Hohov, J. Jaramillo, A. Khalilzadeh, K. Lee, M. Mahdavikhorrami, A. Malara, S. Paredes, L. Pétré, N. Postiau, L. Thomas, M. Vanden Bemden, C. Vander Velde, P. Vanlaer

Ghent University, Ghent, Belgium
M. De Coen, D. Dobur, Y. Hong, J. Knolle, L. Lambrecht, G. Mestdach, C. Rendón, A. Samalan, K. Skovpen, N. Van Den Bossche, L. Wezenbeek

Université Catholique de Louvain, Louvain-la-Neuve, Belgium
A. Benecke, G. Bruno, C. Caputo, C. Delaere, I.S. Donertas, A. Giammanco, K. Jaffel, Sa. Jain, V. Lemaitre, J. Lidrych, P. Mastrapasqua, K. Mondal, T.T. Tran, S. Wertz

Centro Brasileiro de Pesquisas Fisicas, Rio de Janeiro, Brazil
G.A. Alves, E. Coelho, C. Hensel, T. Menezes De Oliveira, A. Moraes, P. Rebello Teles, M. Soeiro

Universidade do Estado do Rio de Janeiro, Rio de Janeiro, Brazil
W.L. Aldá Júnior, M. Alves Gallo Pereira, M. Barroso Ferreira Filho, H. Brandao Malbouisson, W. Carvalho, J. Chinellato[5], E.M. Da Costa, G.G. Da Silveira[6], D. De Jesus Damiao, S. Fonseca De Souza, J. Martins[7], C. Mora Herrera, K. Mota Amarilo, L. Mundim, H. Nogima, A. Santoro, S.M. Silva Do Amaral, A. Sznajder, M. Thiel, A. Vilela Pereira

Universidade Estadual Paulista, Universidade Federal do ABC, São Paulo, Brazil
C.A. Bernardes[6], L. Calligaris, T.R. Fernandez Perez Tomei, E.M. Gregores, P.G. Mercadante, S.F. Novaes, B. Orzari, Sandra S. Padula

Institute for Nuclear Research and Nuclear Energy, Bulgarian Academy of Sciences, Sofia, Bulgaria
A. Aleksandrov, G. Antchev, R. Hadjiiska, P. Iaydjiev, M. Misheva, M. Shopova, G. Sultanov

University of Sofia, Sofia, Bulgaria
A. Dimitrov, T. Ivanov, L. Litov, B. Pavlov, P. Petkov, A. Petrov, E. Shumka

Instituto De Alta Investigación, Universidad de Tarapacá, Casilla 7 D, Arica, Chile
S. Keshri, S.Thakur

Beihang University, Beijing, China
T. Cheng, Q. Guo, T. Javaid, M. Mittal, L. Yuan

Department of Physics, Tsinghua University, Beijing, China
G. Bauer[8,9], Z. Hu, K. Yi[8,10]

Institute of High Energy Physics, Beijing, China
G.M. Chen[11], H.S. Chen[11], M. Chen[11], F. Iemmi, C.H. Jiang, A. Kapoor, H. Liao, Z.-A. Liu[12], F. Monti, M.A. Shahzad[11], R. Sharma, J.N. Song[12], J. Tao, C. Wang[11], J. Wang, Z. Wang[11], H. Zhang

State Key Laboratory of Nuclear Physics and Technology, Peking University, Beijing, China
A. Agapitos, Y. Ban, A. Levin, C. Li, Q. Li, X. Lyu, Y. Mao, S.J. Qian, X. Sun, D. Wang, H. Yang, C. Zhou

Sun Yat-Sen University, Guangzhou, China
Z. You

University of Science and Technology of China, Hefei, China
N. Lu

Institute of Modern Physics and Key Laboratory of Nuclear Physics and Ion-beam Application (MOE) - Fudan University, Shanghai, China
D. Leggat, H. Okawa, Y. Zhang

Zhejiang University, Hangzhou, Zhejiang, China
Z. Lin, C. Lu, M. Xiao

Universidad de Los Andes, Bogota, Colombia
C. Avila, D.A. Barbosa Trujillo, A. Cabrera, C. Florez, J. Fraga, J.A. Reyes Vega

Universidad de Antioquia, Medellin, Colombia
J. Mejia Guisao, F. Ramirez, M. Rodriguez, J.D. Ruiz Alvarez

University of Split, Faculty of Electrical Engineering, Mechanical Engineering and Naval Architecture, Split, Croatia
D. Giljanovic, N. Godinovic, D. Lelas, A. Sculac

University of Split, Faculty of Science, Split, Croatia
M. Kovac, T. Sculac

Institute Rudjer Boskovic, Zagreb, Croatia
P. Bargassa, V. Brigljevic, B.K. Chitroda, D. Ferencek, S. Mishra, A. Starodumov[13], T. Susa

University of Cyprus, Nicosia, Cyprus
A. Attikis, K. Christoforou, S. Konstantinou, J. Mousa, C. Nicolaou, F. Ptochos, P.A. Razis, H. Rykaczewski, H. Saka, A. Stepennov

Charles University, Prague, Czech Republic
M. Finger, M. Finger Jr., A. Kveton

Escuela Politecnica Nacional, Quito, Ecuador
E. Ayala

Universidad San Francisco de Quito, Quito, Ecuador
E. Carrera Jarrin

Academy of Scientific Research and Technology of the Arab Republic of Egypt, Egyptian Network of High Energy Physics, Cairo, Egypt
A.A. Abdelalim[14,15], E. Salama[16,17]

Center for High Energy Physics (CHEP-FU), Fayoum University, El-Fayoum, Egypt
A. Lotfy, M.A. Mahmoud

National Institute of Chemical Physics and Biophysics, Tallinn, Estonia
R.K. Dewanjee[18], K. Ehataht, M. Kadastik, T. Lange, S. Nandan, C. Nielsen, J. Pata, M. Raidal, L. Tani, C. Veelken

Department of Physics, University of Helsinki, Helsinki, Finland
H. Kirschenmann, K. Osterberg, M. Voutilainen

Helsinki Institute of Physics, Helsinki, Finland
S. Bharthuar, E. Brücken, F. Garcia, J. Havukainen, K.T.S. Kallonen, M.S. Kim, R. Kinnunen, T. Lampén, K. Lassila-Perini, S. Lehti, T. Lindén, M. Lotti, L. Martikainen, M. Myllymäki, M.m. Rantanen, H. Siikonen, E. Tuominen, J. Tuominiemi

Lappeenranta-Lahti University of Technology, Lappeenranta, Finland
P. Luukka, H. Petrow, T. Tuuva[†]

IRFU, CEA, Université Paris-Saclay, Gif-sur-Yvette, France
M. Besancon, F. Couderc, M. Dejardin, D. Denegri, J.L. Faure, F. Ferri, S. Ganjour, P. Gras, G. Hamel de Monchenault, V. Lohezic, J. Malcles, J. Rander, A. Rosowsky, M.Ö. Sahin, A. Savoy-Navarro[19], P. Simkina, M. Titov

Laboratoire Leprince-Ringuet, CNRS/IN2P3, Ecole Polytechnique, Institut Polytechnique de Paris, Palaiseau, France
C. Baldenegro Barrera, F. Beaudette, A. Buchot Perraguin, P. Busson, A. Cappati, C. Charlot, F. Damas, O. Davignon, A. De Wit, G. Falmagne, B.A. Fontana Santos Alves, S. Ghosh, A. Gilbert, R. Granier de Cassagnac, A. Hakimi, B. Harikrishnan, L. Kalipoliti, G. Liu, J. Motta, M. Nguyen, C. Ochando, L. Portales, R. Salerno, U. Sarkar, J.B. Sauvan, Y. Sirois, A. Tarabini, E. Vernazza, A. Zabi, A. Zghiche

Université de Strasbourg, CNRS, IPHC UMR 7178, Strasbourg, France
J.-L. Agram[20], J. Andrea, D. Apparu, D. Bloch, J.-M. Brom, E.C. Chabert, C. Collard, S. Falke, U. Goerlach, C. Grimault, R. Haeberle, A.-C. Le Bihan, M.A. Sessini, P. Van Hove

Institut de Physique des 2 Infinis de Lyon (IP2I), Villeurbanne, France
S. Beauceron, B. Blancon, G. Boudoul, N. Chanon, J. Choi, D. Contardo, P. Depasse, C. Dozen[21], H. El Mamouni, J. Fay, S. Gascon, M. Gouzevitch, C. Greenberg, G. Grenier, B. Ille, I.B. Laktineh, M. Lethuillier, L. Mirabito, S. Perries, M. Vander Donckt, P. Verdier, J. Xiao

Georgian Technical University, Tbilisi, Georgia
G. Adamov, I. Lomidze, Z. Tsamalaidze[13]

RWTH Aachen University, I. Physikalisches Institut, Aachen, Germany

V. Botta, L. Feld, K. Klein, M. Lipinski, D. Meuser, A. Pauls, N. Röwert, M. Teroerde

RWTH Aachen University, III. Physikalisches Institut A, Aachen, Germany
S. Diekmann, A. Dodonova, N. Eich, D. Eliseev, F. Engelke, M. Erdmann, P. Fackeldey, B. Fischer, T. Hebbeker, K. Hoepfner, F. Ivone, A. Jung, M.y. Lee, L. Mastrolorenzo, M. Merschmeyer, A. Meyer, S. Mukherjee, D. Noll, A. Novak, F. Nowotny, A. Pozdnyakov, Y. Rath, W. Redjeb, F. Rehm, H. Reithler, V. Sarkisovi, A. Schmidt, S.C. Schuler, A. Sharma, A. Stein, F. Torres Da Silva De Araujo[22], L. Vigilante, S. Wiedenbeck, S. Zaleski

RWTH Aachen University, III. Physikalisches Institut B, Aachen, Germany
C. Dziwok, G. Flügge, W. Haj Ahmad[23], T. Kress, A. Nowack, O. Pooth, A. Stahl, T. Ziemons, A. Zotz

Deutsches Elektronen-Synchrotron, Hamburg, Germany
H. Aarup Petersen, M. Aldaya Martin, J. Alimena, S. Amoroso, Y. An, S. Baxter, M. Bayatmakou, H. Becerril Gonzalez, O. Behnke, A. Belvedere, S. Bhattacharya, F. Blekman[24], K. Borras[25], D. Brunner, A. Campbell, A. Cardini, C. Cheng, F. Colombina, S. Consuegra Rodríguez, G. Correia Silva, M. De Silva, G. Eckerlin, D. Eckstein, L.I. Estevez Banos, O. Filatov, E. Gallo[24], A. Geiser, A. Giraldi, G. Greau, V. Guglielmi, M. Guthoff, A. Hinzmann, A. Jafari[26], L. Jeppe, N.Z. Jomhari, B. Kaech, M. Kasemann, H. Kaveh, C. Kleinwort, R. Kogler, M. Komm, D. Krücker, W. Lange, D. Leyva Pernia, K. Lipka[27], W. Lohmann[28], R. Mankel, I.-A. Melzer-Pellmann, M. Mendizabal Morentin, J. Metwally, A.B. Meyer, G. Milella, A. Mussgiller, A. Nürnberg, Y. Otarid, D. Pérez Adán, E. Ranken, A. Raspereza, B. Ribeiro Lopes, J. Rübenach, A. Saggio, M. Scham[29,25], V. Scheurer, S. Schnake[25], P. Schütze, C. Schwanenberger[24], D. Selivanova, M. Shchedrolosiev, R.E. Sosa Ricardo, L.P. Sreelatha Pramod, D. Stafford, F. Vazzoler, A. Ventura Barroso, R. Walsh, Q. Wang, Y. Wen, K. Wichmann, L. Wiens[25], C. Wissing, S. Wuchterl, Y. Yang, A. Zimermmane Castro Santos

University of Hamburg, Hamburg, Germany
A. Albrecht, S. Albrecht, M. Antonello, S. Bein, L. Benato, M. Bonanomi, P. Connor, M. Eich, K. El Morabit, Y. Fischer, A. Fröhlich, C. Garbers, E. Garutti, A. Grohsjean, M. Hajheidari, J. Haller, H.R. Jabusch, G. Kasieczka, P. Keicher, R. Klanner, W. Korcari, T. Kramer, V. Kutzner, F. Labe, J. Lange, A. Lobanov, C. Matthies, A. Mehta, L. Moureaux, M. Mrowietz, A. Nigamova, Y. Nissan, A. Paasch, K.J. Pena Rodriguez, T. Quadfasel, B. Raciti, M. Rieger, D. Savoiu, J. Schindler, P. Schleper, M. Schröder, J. Schwandt, M. Sommerhalder, H. Stadie, G. Steinbrück, A. Tews, M. Wolf

Karlsruher Institut fuer Technologie, Karlsruhe, Germany
S. Brommer, M. Burkart, E. Butz, T. Chwalek, A. Dierlamm, A. Droll, N. Faltermann, M. Giffels, A. Gottmann, F. Hartmann[30], R. Hofsaess, M. Horzela, U. Husemann, M. Klute, R. Koppenhöfer, M. Link, A. Lintuluoto, S. Maier, S. Mitra, M. Mormile, Th. Müller, M. Neukum, M. Oh, G. Quast, K. Rabbertz, B. Regnery, N. Shadskiy, I. Shvetsov, H.J. Simonis, N. Trevisani, R. Ulrich, J. van der Linden, R.F. Von Cube, M. Wassmer, S. Wieland, F. Wittig, R. Wolf, S. Wunsch, X. Zuo

Institute of Nuclear and Particle Physics (INPP), NCSR Demokritos, Aghia Paraskevi,

Greece
G. Anagnostou, P. Assiouras, G. Daskalakis, A. Kyriakis, A. Papadopoulos[30], A. Stakia

National and Kapodistrian University of Athens, Athens, Greece
D. Karasavvas, P. Kontaxakis, G. Melachroinos, A. Panagiotou, I. Papavergou, I. Paraskevas, N. Saoulidou, K. Theofilatos, E. Tziaferi, K. Vellidis, I. Zisopoulos

National Technical University of Athens, Athens, Greece
G. Bakas, T. Chatzistavrou, G. Karapostoli, K. Kousouris, I. Papakrivopoulos, E. Siamarkou, G. Tsipolitis, A. Zacharopoulou

University of Ioánnina, Ioánnina, Greece
K. Adamidis, I. Bestintzanos, I. Evangelou, C. Foudas, P. Gianneios, C. Kamtsikis, P. Katsoulis, P. Kokkas, P.G. Kosmoglou Kioseoglou, N. Manthos, I. Papadopoulos, J. Strologas

MTA-ELTE Lendület CMS Particle and Nuclear Physics Group, Eötvös Loránd University, Budapest, Hungary
M. Csanád, K. Farkas, M.M.A. Gadallah[31], Á. Kadlecsik, P. Major, K. Mandal, G. Pásztor, A.J. Rádl[32], G.I. Veres

Wigner Research Centre for Physics, Budapest, Hungary
M. Bartók[33], C. Hajdu, D. Horvath[34,35], F. Sikler, V. Veszpremi

Faculty of Informatics, University of Debrecen, Debrecen, Hungary
P. Raics, B. Ujvari[36], G. Zilizi

Institute of Nuclear Research ATOMKI, Debrecen, Hungary
G. Bencze, S. Czellar, J. Karancsi[33], J. Molnar, Z. Szillasi

Karoly Robert Campus, MATE Institute of Technology, Gyongyos, Hungary
T. Csorgo[32], F. Nemes[32], T. Novak

Panjab University, Chandigarh, India
J. Babbar, S. Bansal, S.B. Beri, V. Bhatnagar, G. Chaudhary, S. Chauhan, N. Dhingra[37], R. Gupta, A. Kaur, A. Kaur, H. Kaur, M. Kaur, S. Kumar, P. Kumari, M. Meena, K. Sandeep, T. Sheokand, J.B. Singh[38], A. Singla

University of Delhi, Delhi, India
A. Ahmed, A. Bhardwaj, A. Chhetri, B.C. Choudhary, A. Kumar, M. Naimuddin, K. Ranjan, S. Saumya

Saha Institute of Nuclear Physics, HBNI, Kolkata, India
S. Acharya, S. Baradia, S. Barman[39], S. Bhattacharya, D. Bhowmik, S. Dutta, S. Dutta, B. Gomber[40], P. Palit, G. Saha, B. Sahu[40], S. Sarkar

Indian Institute of Technology Madras, Madras, India
M.M. Ameen, P.K. Behera, S.C. Behera, S. Chatterjee, P. Jana, P. Kalbhor, J.R. Komaragiri[41], D. Kumar[41], L. Panwar[41], R. Pradhan, P.R. Pujahari, N.R. Saha, A. Sharma, A.K. Sikdar, S. Verma

Tata Institute of Fundamental Research-A, Mumbai, India
T. Aziz, I. Das, S. Dugad, M. Kumar, G.B. Mohanty, P. Suryadevara

Tata Institute of Fundamental Research-B, Mumbai, India
A. Bala, S. Banerjee, R.M. Chatterjee, M. Guchait, S. Karmakar, S. Kumar,

G. Majumder, K. Mazumdar, S. Mukherjee, A. Thachayath

National Institute of Science Education and Research, An OCC of Homi Bhabha National Institute, Bhubaneswar, Odisha, India
S. Bahinipati[42], A.K. Das, C. Kar, D. Maity[43], P. Mal, T. Mishra, V.K. Muraleedharan Nair Bindhu[43], K. Naskar[43], A. Nayak[43], P. Sadangi, P. Saha, S.K. Swain, S. Varghese[43], D. Vats[43]

Indian Institute of Science Education and Research (IISER), Pune, India
A. Alpana, S. Dube, B. Kansal, A. Laha, A. Rastogi, S. Sharma

Isfahan University of Technology, Isfahan, Iran
H. Bakhshiansohi[44], E. Khazaie[45], M. Zeinali[46]

Institute for Research in Fundamental Sciences (IPM), Tehran, Iran
S. Chenarani[47], S.M. Etesami, M. Khakzad, M. Mohammadi Najafabadi

University College Dublin, Dublin, Ireland
M. Grunewald

INFN Sezione di Bari[a], Università di Bari[b], Politecnico di Bari[c], Bari, Italy
M. Abbrescia[a,b], R. Aly[a,c,14], A. Colaleo[a,b], D. Creanza[a,c], B. D′ Anzi[a,b], N. De Filippis[a,c], M. De Palma[a,b], A. Di Florio[a,c], W. Elmetenawee[a,b,14], L. Fiore[a], G. Iaselli[a,c], G. Maggi[a,c], M. Maggi[a], I. Margjeka[a,b], V. Mastrapasqua[a,b], S. My[a,b], S. Nuzzo[a,b], A. Pellecchia[a,b], A. Pompili[a,b], G. Pugliese[a,c], R. Radogna[a], G. Ramirez-Sanchez[a,c], D. Ramos[a], A. Ranieri[a], L. Silvestris[a], F.M. Simone[a,b], Ü. Sözbilir[a], A. Stamerra[a], R. Venditti[a], P. Verwilligen[a], A. Zaza[a,b]

INFN Sezione di Bologna[a], Università di Bologna[b], Bologna, Italy
G. Abbiendi[a], C. Battilana[a,b], D. Bonacorsi[a,b], L. Borgonovi[a], R. Campanini[a,b], P. Capiluppi[a,b], A. Castro[a,b], F.R. Cavallo[a], M. Cuffiani[a,b], T. Diotalevi[a,b], F. Fabbri[a], A. Fanfani[a,b], D. Fasanella[a,b], P. Giacomelli[a], L. Giommi[a,b], C. Grandi[a], L. Guiducci[a,b], S. Lo Meo[a,48], L. Lunerti[a,b], S. Marcellini[a], G. Masetti[a], F.L. Navarria[a,b], A. Perrotta[a], F. Primavera[a,b], A.M. Rossi[a,b], T. Rovelli[a,b], G.P. Siroli[a,b]

INFN Sezione di Catania[a], Università di Catania[b], Catania, Italy
S. Costa[a,b,49], A. Di Mattia[a], R. Potenza[a,b], A. Tricomi[a,b,49], C. Tuve[a,b]

INFN Sezione di Firenze[a], Università di Firenze[b], Firenze, Italy
G. Barbagli[a], G. Bardelli[a,b], B. Camaiani[a,b], A. Cassese[a], R. Ceccarelli[a], V. Ciulli[a,b], C. Civinini[a], R. D'Alessandro[a,b], E. Focardi[a,b], G. Latino[a,b], P. Lenzi[a,b], M. Lizzo[a], M. Meschini[a], S. Paoletti[a], A. Papanastassiou[a,b], G. Sguazzoni[a], L. Viliani[a]

INFN Laboratori Nazionali di Frascati, Frascati, Italy
L. Benussi, S. Bianco, S. Meola[50], D. Piccolo

INFN Sezione di Genova[a], Università di Genova[b], Genova, Italy
P. Chatagnon[a], F. Ferro[a], E. Robutti[a], S. Tosi[a,b]

INFN Sezione di Milano-Bicocca[a], Università di Milano-Bicocca[b], Milano, Italy
A. Benaglia[a], G. Boldrini[a], F. Brivio[a], F. Cetorelli[a], F. De Guio[a,b], M.E. Dinardo[a,b], P. Dini[a], S. Gennai[a], A. Ghezzi[a,b], P. Govoni[a,b], L. Guzzi[a],

M.T. Lucchini[a,b], M. Malberti[a], S. Malvezzi[a], A. Massironi[a], D. Menasce[a], L. Moroni[a], M. Paganoni[a,b], D. Pedrini[a], B.S. Pinolini[a], S. Ragazzi[a,b], N. Redaelli[a], T. Tabarelli de Fatis[a,b], D. Zuolo[a]

INFN Sezione di Napoli[a], Università di Napoli 'Federico II'[b], Napoli, Italy; Università della Basilicata[c], Potenza, Italy; Università G. Marconi[d], Roma, Italy
S. Buontempo[a], A. Cagnotta[a,b], F. Carnevali[a,b], N. Cavallo[a,c], A. De Iorio[a,b], F. Fabozzi[a,c], A.O.M. Iorio[a,b], L. Lista[a,b,51], P. Paolucci[a,30], B. Rossi[a], C. Sciacca[a,b]

INFN Sezione di Padova[a], Università di Padova[b], Padova, Italy; Università di Trento[c], Trento, Italy
R. Ardino[a], P. Azzi[a], N. Bacchetta[a,52], D. Bisello[a,b], P. Bortignon[a], A. Bragagnolo[a,b], R. Carlin[a,b], P. Checchia[a], T. Dorigo[a], F. Gasparini[a,b], U. Gasparini[a,b], G. Govi[a], G. Grosso[a], L. Layer[a,53], E. Lusiani[a], M. Margoni[a,b], A.T. Meneguzzo[a,b], M. Migliorini[a,b], J. Pazzini[a,b], P. Ronchese[a,b], R. Rossin[a,b], G. Strong[a], M. Tosi[a,b], A. Triossi[a,b], S. Ventura[a], H. Yarar[a,b], M. Zanetti[a,b], P. Zotto[a,b], A. Zucchetta[a,b], G. Zumerle[a,b]

INFN Sezione di Pavia[a], Università di Pavia[b], Pavia, Italy
S. Abu Zeid[a,17], C. Aimè[a,b], A. Braghieri[a], S. Calzaferri[a,b], D. Fiorina[a,b], P. Montagna[a,b], V. Re[a], C. Riccardi[a,b], P. Salvini[a], I. Vai[a,b], P. Vitulo[a,b]

INFN Sezione di Perugia[a], Università di Perugia[b], Perugia, Italy
S. Ajmal[a,b], P. Asenov[a,54], G.M. Bilei[a], D. Ciangottini[a,b], L. Fanò[a,b], M. Magherini[a,b], G. Mantovani[a,b], V. Mariani[a,b], M. Menichelli[a], F. Moscatelli[a,54], A. Piccinelli[a,b], M. Presilla[a,b], A. Rossi[a,b], A. Santocchia[a,b], D. Spiga[a], T. Tedeschi[a,b]

INFN Sezione di Pisa[a], Università di Pisa[b], Scuola Normale Superiore di Pisa[c], Pisa, Italy; Università di Siena[d], Siena, Italy
P. Azzurri[a], G. Bagliesi[a], R. Bhattacharya[a], L. Bianchini[a,b], T. Boccali[a], E. Bossini[a], D. Bruschini[a,c], R. Castaldi[a], M.A. Ciocci[a,b], M. Cipriani[a,b], V. D'Amante[a,d], R. Dell'Orso[a], S. Donato[a], A. Giassi[a], F. Ligabue[a,c], D. Matos Figueiredo[a], A. Messineo[a,b], M. Musich[a,b], F. Palla[a], S. Parolia[a], A. Rizzi[a,b], G. Rolandi[a,c], S. Roy Chowdhury[a], T. Sarkar[a], A. Scribano[a], P. Spagnolo[a], R. Tenchini[a,b], G. Tonelli[a,b], N. Turini[a,d], A. Venturi[a], P.G. Verdini[a]

INFN Sezione di Roma[a], Sapienza Università di Roma[b], Roma, Italy
P. Barria[a], M. Campana[a,b], F. Cavallari[a], L. Cunqueiro Mendez[a,b], D. Del Re[a,b], E. Di Marco[a], M. Diemoz[a], F. Errico[a,b], E. Longo[a,b], P. Meridiani[a], J. Mijuskovic[a,b], G. Organtini[a,b], F. Pandolfi[a], R. Paramatti[a,b], C. Quaranta[a,b], S. Rahatlou[a,b], C. Rovelli[a], F. Santanastasio[a,b], L. Soffi[a], R. Tramontano[a,b]

INFN Sezione di Torino[a], Università di Torino[b], Torino, Italy; Università del Piemonte Orientale[c], Novara, Italy
N. Amapane[a,b], R. Arcidiacono[a,c], S. Argiro[a,b], M. Arneodo[a,c], N. Bartosik[a], R. Bellan[a,b], A. Bellora[a,b], C. Biino[a], N. Cartiglia[a], M. Costa[a,b], R. Covarelli[a,b], N. Demaria[a], L. Finco[a], M. Grippo[a,b], B. Kiani[a,b], F. Legger[a], F. Luongo[a,b], C. Mariotti[a], S. Maselli[a], A. Mecca[a,b], E. Migliore[a,b], M. Monteno[a], R. Mulargia[a], M.M. Obertino[a,b], G. Ortona[a], L. Pacher[a,b], N. Pastrone[a], M. Pelliccioni[a], M. Ruspa[a,c], F. Siviero[a,b], V. Sola[a,b], A. Solano[a,b], D. Soldi[a,b],

A. Staiano[a], C. Tarricone[a,b], M. Tornago[a,b], D. Trocino[a], G. Umoret[a,b], E. Vlasov[a,b]

INFN Sezione di Trieste[a], Università di Trieste[b], Trieste, Italy
S. Belforte[a], V. Candelise[a,b], M. Casarsa[a], F. Cossutti[a], K. De Leo[a,b], G. Della Ricca[a,b]

Kyungpook National University, Daegu, Korea
S. Dogra, J. Hong, C. Huh, B. Kim, D.H. Kim, J. Kim, H. Lee, S.W. Lee, C.S. Moon, Y.D. Oh, S.I. Pak, M.S. Ryu, S. Sekmen, Y.C. Yang

Chonnam National University, Institute for Universe and Elementary Particles, Kwangju, Korea
G. Bak, P. Gwak, H. Kim, D.H. Moon

Hanyang University, Seoul, Korea
E. Asilar, D. Kim, T.J. Kim, J.A. Merlin, J. Park

Korea University, Seoul, Korea
S. Choi, S. Han, B. Hong, K. Lee, K.S. Lee, S. Lee, J. Park, S.K. Park, J. Yoo

Kyung Hee University, Department of Physics, Seoul, Korea
J. Goh

Sejong University, Seoul, Korea
H. S. Kim, Y. Kim, S. Lee

Seoul National University, Seoul, Korea
J. Almond, J.H. Bhyun, J. Choi, W. Jun, J. Kim, J.S. Kim, S. Ko, H. Kwon, H. Lee, J. Lee, J. Lee, S. Lee, B.H. Oh, S.B. Oh, H. Seo, U.K. Yang, I. Yoon

University of Seoul, Seoul, Korea
W. Jang, D.Y. Kang, Y. Kang, S. Kim, B. Ko, J.S.H. Lee, Y. Lee, I.C. Park, Y. Roh, Watson, I.J., S. Yang

Yonsei University, Department of Physics, Seoul, Korea
S. Ha, H.D. Yoo

Sungkyunkwan University, Suwon, Korea
M. Choi, M.R. Kim, H. Lee, Y. Lee, I. Yu

College of Engineering and Technology, American University of the Middle East (AUM), Dasman, Kuwait
T. Beyrouthy, Y. Maghrbi

Riga Technical University, Riga, Latvia
K. Dreimanis, A. Gaile, G. Pikurs, A. Potrebko, M. Seidel, V. Veckalns[55]

University of Latvia (LU), Riga, Latvia
N.R. Strautnieks

Vilnius University, Vilnius, Lithuania
M. Ambrozas, A. Juodagalvis, A. Rinkevicius, G. Tamulaitis

National Centre for Particle Physics, Universiti Malaya, Kuala Lumpur, Malaysia
N. Bin Norjoharuddeen, I. Yusuff[56], Z. Zolkapli

Universidad de Sonora (UNISON), Hermosillo, Mexico

J.F. Benitez, A. Castaneda Hernandez, H.A. Encinas Acosta, L.G. Gallegos Maríñez, M. León Coello, J.A. Murillo Quijada, A. Sehrawat, L. Valencia Palomo

Centro de Investigacion y de Estudios Avanzados del IPN, Mexico City, Mexico
G. Ayala, H. Castilla-Valdez, E. De La Cruz-Burelo, I. Heredia-De La Cruz[57], R. Lopez-Fernandez, C.A. Mondragon Herrera, A. Sánchez Hernández

Universidad Iberoamericana, Mexico City, Mexico
C. Oropeza Barrera, M. Ramírez García

Benemerita Universidad Autonoma de Puebla, Puebla, Mexico
I. Bautista, I. Pedraza, H.A. Salazar Ibarguen, C. Uribe Estrada

University of Montenegro, Podgorica, Montenegro
I. Bubanja, N. Raicevic

University of Canterbury, Christchurch, New Zealand
P.H. Butler

National Centre for Physics, Quaid-I-Azam University, Islamabad, Pakistan
A. Ahmad, M.I. Asghar, A. Awais, M.I.M. Awan, H.R. Hoorani, W.A. Khan

AGH University of Science and Technology Faculty of Computer Science, Electronics and Telecommunications, Krakow, Poland
V. Avati, L. Grzanka, M. Malawski

National Centre for Nuclear Research, Swierk, Poland
H. Bialkowska, M. Bluj, B. Boimska, M. Górski, M. Kazana, M. Szleper, P. Zalewski

Institute of Experimental Physics, Faculty of Physics, University of Warsaw, Warsaw, Poland
K. Bunkowski, K. Doroba, A. Kalinowski, M. Konecki, J. Krolikowski, A. Muhammad

Laboratório de Instrumentação e Física Experimental de Partículas, Lisboa, Portugal
M. Araujo, D. Bastos, C. Beirão Da Cruz E Silva, A. Boletti, M. Bozzo, P. Faccioli, M. Gallinaro, J. Hollar, N. Leonardo, T. Niknejad, A. Petrilli, M. Pisano, J. Seixas, J. Varela

Faculty of Physics, University of Belgrade, Belgrade, Serbia
P. Adzic, P. Milenovic

VINCA Institute of Nuclear Sciences, University of Belgrade, Belgrade, Serbia
M. Dordevic, J. Milosevic, V. Rekovic

Centro de Investigaciones Energéticas Medioambientales y Tecnológicas (CIEMAT), Madrid, Spain
M. Aguilar-Benitez, J. Alcaraz Maestre, M. Barrio Luna, Cristina F. Bedoya, M. Cepeda, M. Cerrada, N. Colino, B. De La Cruz, A. Delgado Peris, D. Fernández Del Val, J.P. Fernández Ramos, J. Flix, M.C. Fouz, O. Gonzalez Lopez, S. Goy Lopez, J.M. Hernandez, M.I. Josa, J. León Holgado, D. Moran, C. M. Morcillo Perez, Á. Navarro Tobar, C. Perez Dengra, A. Pérez-Calero Yzquierdo, J. Puerta Pelayo, I. Redondo, D.D. Redondo Ferrero, L. Romero, S. Sánchez Navas, L. Urda Gómez, J. Vazquez Escobar, C. Willmott

Universidad Autónoma de Madrid, Madrid, Spain

J.F. de Trocóniz

Universidad de Oviedo, Instituto Universitario de Ciencias y Tecnologías Espaciales de Asturias (ICTEA), Oviedo, Spain
B. Alvarez Gonzalez, J. Cuevas, J. Fernandez Menendez, S. Folgueras, I. Gonzalez Caballero, J.R. González Fernández, E. Palencia Cortezon, C. Ramón Álvarez, V. Rodríguez Bouza, A. Soto Rodríguez, A. Trapote, C. Vico Villalba, P. Vischia

Instituto de Física de Cantabria (IFCA), CSIC-Universidad de Cantabria, Santander, Spain
S. Blanco Fernández, J.A. Brochero Cifuentes, I.J. Cabrillo, A. Calderon, J. Duarte Campderros, M. Fernandez, C. Fernandez Madrazo, G. Gomez, C. Lasaosa García, C. Martinez Rivero, P. Martinez Ruiz del Arbol, F. Matorras, P. Matorras Cuevas, E. Navarrete Ramos, J. Piedra Gomez, C. Prieels, L. Scodellaro, I. Vila, J.M. Vizan Garcia

University of Colombo, Colombo, Sri Lanka
M.K. Jayananda, B. Kailasapathy[58], D.U.J. Sonnadara, D.D.C. Wickramarathna

University of Ruhuna, Department of Physics, Matara, Sri Lanka
W.G.D. Dharmaratna, K. Liyanage, N. Perera, N. Wickramage

CERN, European Organization for Nuclear Research, Geneva, Switzerland
D. Abbaneo, C. Amendola, E. Auffray, G. Auzinger, J. Baechler, D. Barney, A. Bermúdez Martínez, M. Bianco, B. Bilin, A.A. Bin Anuar, A. Bocci, E. Brondolin, C. Caillol, T. Camporesi, G. Cerminara, N. Chernyavskaya, D. d'Enterria, A. Dabrowski, A. David, A. De Roeck, M.M. Defranchis, M. Deile, M. Dobson, F. Fallavollita[59], L. Forthomme, G. Franzoni, W. Funk, S. Giani, D. Gigi, K. Gill, F. Glege, L. Gouskos, M. Haranko, J. Hegeman, V. Innocente, T. James, P. Janot, J. Kieseler, S. Laurila, P. Lecoq, E. Leutgeb, C. Lourenço, B. Maier, L. Malgeri, M. Mannelli, A.C. Marini, F. Meijers, S. Mersi, E. Meschi, V. Milosevic, F. Moortgat, M. Mulders, S. Orfanelli, F. Pantaleo, M. Peruzzi, G. Petrucciani, A. Pfeiffer, M. Pierini, D. Piparo, H. Qu, D. Rabady, G. Reales Gutiérrez, M. Rovere, H. Sakulin, S. Scarfi, M. Selvaggi, A. Sharma, K. Shchelina, P. Silva, P. Sphicas[60], A.G. Stahl Leiton, A. Steen, S. Summers, D. Treille, P. Tropea, A. Tsirou, D. Walter, J. Wanczyk[61], K.A. Wozniak[62], P. Zehetner, P. Zejdl, W.D. Zeuner

Paul Scherrer Institut, Villigen, Switzerland
T. Bevilacqua[63], L. Caminada[63], A. Ebrahimi, W. Erdmann, R. Horisberger, Q. Ingram, H.C. Kaestli, D. Kotlinski, C. Lange, M. Missiroli[63], L. Noehte[63], T. Rohe

ETH Zurich - Institute for Particle Physics and Astrophysics (IPA), Zurich, Switzerland
T.K. Aarrestad, K. Androsov[61], M. Backhaus, A. Calandri, C. Cazzaniga, K. Datta, A. De Cosa, G. Dissertori, M. Dittmar, M. Donegà, F. Eble, M. Galli, K. Gedia, F. Glessgen, C. Grab, D. Hits, W. Lustermann, A.-M. Lyon, R.A. Manzoni, M. Marchegiani, L. Marchese, C. Martin Perez, A. Mascellani[61], F. Nessi-Tedaldi, F. Pauss, V. Perovic, S. Pigazzini, M.G. Ratti, M. Reichmann, C. Reissel, T. Reitenspiess, B. Ristic, F. Riti, D. Ruini, D.A. Sanz Becerra, R. Seidita, J. Steggemann[61], D. Valsecchi, R. Wallny

Universität Zürich, Zurich, Switzerland
C. Amsler[64], P. Bärtschi, C. Botta, D. Brzhechko, M.F. Canelli, K. Cormier,

R. Del Burgo, J.K. Heikkilä, M. Huwiler, W. Jin, A. Jofrehei, B. Kilminster, S. Leontsinis, S.P. Liechti, A. Macchiolo, P. Meiring, V.M. Mikuni, U. Molinatti, I. Neutelings, A. Reimers, P. Robmann, S. Sanchez Cruz, K. Schweiger, M. Senger, Y. Takahashi

National Central University, Chung-Li, Taiwan
C. Adloff[65], C.M. Kuo, W. Lin, P.K. Rout, P.C. Tiwari[41], S.S. Yu

National Taiwan University (NTU), Taipei, Taiwan
L. Ceard, Y. Chao, K.F. Chen, P.s. Chen, Z.g. Chen, W.-S. Hou, T.h. Hsu, Y.w. Kao, R. Khurana, G. Kole, Y.y. Li, R.-S. Lu, E. Paganis, A. Psallidas, X.f. Su, J. Thomas-Wilsker, H.y. Wu, E. Yazgan

Chulalongkorn University, Faculty of Science, Department of Physics, Bangkok, Thailand
C. Asawatangtrakuldee, N. Srimanobhas, V. Wachirapusitanand

Çukurova University, Physics Department, Science and Art Faculty, Adana, Turkey
D. Agyel, F. Boran, Z.S. Demiroglu, F. Dolek, I. Dumanoglu[66], E. Eskut, Y. Guler[67], E. Gurpinar Guler[67], C. Isik, O. Kara, A. Kayis Topaksu, U. Kiminsu, G. Onengut, K. Ozdemir[68], A. Polatoz, B. Tali[69], U.G. Tok, S. Turkcapar, E. Uslan, I.S. Zorbakir

Middle East Technical University, Physics Department, Ankara, Turkey
K. Ocalan[70], M. Yalvac[71]

Bogazici University, Istanbul, Turkey
B. Akgun, I.O. Atakisi, E. Gülmez, M. Kaya[72], O. Kaya[73], S. Tekten[74]

Istanbul Technical University, Istanbul, Turkey
A. Cakir, K. Cankocak[66], Y. Komurcu, S. Sen[75]

Istanbul University, Istanbul, Turkey
O. Aydilek, S. Cerci[69], V. Epshteyn, B. Hacisahinoglu, I. Hos[76], B. Isildak[77], B. Kaynak, S. Ozkorucuklu, O. Potok, H. Sert, C. Simsek, D. Sunar Cerci[69], C. Zorbilmez

Institute for Scintillation Materials of National Academy of Science of Ukraine, Kharkiv, Ukraine
A. Boyaryntsev, B. Grynyov

National Science Centre, Kharkiv Institute of Physics and Technology, Kharkiv, Ukraine
L. Levchuk

University of Bristol, Bristol, United Kingdom
D. Anthony, J.J. Brooke, A. Bundock, F. Bury, E. Clement, D. Cussans, H. Flacher, M. Glowacki, J. Goldstein, H.F. Heath, L. Kreczko, B. Krikler, S. Paramesvaran, S. Seif El Nasr-Storey, V.J. Smith, N. Stylianou[78], K. Walkingshaw Pass, R. White

Rutherford Appleton Laboratory, Didcot, United Kingdom
A.H. Ball, K.W. Bell, A. Belyaev[79], C. Brew, R.M. Brown, D.J.A. Cockerill, C. Cooke, K.V. Ellis, K. Harder, S. Harper, M.-L. Holmberg[80], Sh. Jain, J. Linacre, K. Manolopoulos, D.M. Newbold, E. Olaiya, D. Petyt, T. Reis, G. Salvi, T. Schuh, C.H. Shepherd-Themistocleous, I.R. Tomalin, T. Williams

Imperial College, London, United Kingdom

R. Bainbridge, P. Bloch, C.E. Brown, O. Buchmuller, V. Cacchio, C.A. Carrillo Montoya, G.S. Chahal[81], D. Colling, J.S. Dancu, P. Dauncey, G. Davies, J. Davies, M. Della Negra, S. Fayer, G. Fedi, G. Hall, M.H. Hassanshahi, A. Howard, G. Iles, M. Knight, J. Langford, L. Lyons, A.-M. Magnan, S. Malik, A. Martelli, M. Mieskolainen, J. Nash[82], M. Pesaresi, B.C. Radburn-Smith, A. Richards, A. Rose, C. Seez, R. Shukla, A. Tapper, K. Uchida, G.P. Uttley, L.H. Vage, T. Virdee[30], M. Vojinovic, N. Wardle, D. Winterbottom

Brunel University, Uxbridge, United Kingdom
K. Coldham, J.E. Cole, A. Khan, P. Kyberd, I.D. Reid

Baylor University, Waco, Texas, USA
S. Abdullin, A. Brinkerhoff, B. Caraway, J. Dittmann, K. Hatakeyama, J. Hiltbrand, A.R. Kanuganti, B. McMaster, M. Saunders, S. Sawant, C. Sutantawibul, M. Toms[83], J. Wilson

Catholic University of America, Washington, DC, USA
R. Bartek, A. Dominguez, C. Huerta Escamilla, A.E. Simsek, R. Uniyal, A.M. Vargas Hernandez

The University of Alabama, Tuscaloosa, Alabama, USA
R. Chudasama, S.I. Cooper, S.V. Gleyzer, C.U. Perez, P. Rumerio[84], E. Usai, C. West, R. Yi

Boston University, Boston, Massachusetts, USA
A. Akpinar, A. Albert, D. Arcaro, C. Cosby, Z. Demiragli, C. Erice, E. Fontanesi, D. Gastler, S. Jeon, J. Rohlf, K. Salyer, D. Sperka, D. Spitzbart, I. Suarez, A. Tsatsos, S. Yuan

Brown University, Providence, Rhode Island, USA
G. Benelli, X. Coubez[25], D. Cutts, M. Hadley, U. Heintz, J.M. Hogan[85], T. Kwon, G. Landsberg, K.T. Lau, D. Li, J. Luo, S. Mondal, M. Narain[†], N. Pervan, S. Sagir[86], F. Simpson, M. Stamenkovic, W.Y. Wong, X. Yan, W. Zhang

University of California, Davis, Davis, California, USA
S. Abbott, J. Bonilla, C. Brainerd, R. Breedon, M. Calderon De La Barca Sanchez, M. Chertok, M. Citron, J. Conway, P.T. Cox, R. Erbacher, G. Haza, F. Jensen, O. Kukral, G. Mocellin, M. Mulhearn, D. Pellett, W. Wei, Y. Yao, F. Zhang

University of California, Los Angeles, California, USA
M. Bachtis, R. Cousins, A. Datta, J. Hauser, M. Ignatenko, M.A. Iqbal, T. Lam, E. Manca, W.A. Nash, D. Saltzberg, B. Stone, V. Valuev

University of California, Riverside, Riverside, California, USA
R. Clare, M. Gordon, G. Hanson, W. Si, S. Wimpenny[†]

University of California, San Diego, La Jolla, California, USA
J.G. Branson, S. Cittolin, S. Cooperstein, D. Diaz, J. Duarte, R. Gerosa, L. Giannini, J. Guiang, R. Kansal, V. Krutelyov, R. Lee, J. Letts, M. Masciovecchio, F. Mokhtar, M. Pieri, M. Quinnan, B.V. Sathia Narayanan, V. Sharma, M. Tadel, E. Vourliotis, F. Würthwein, Y. Xiang, A. Yagil

University of California, Santa Barbara - Department of Physics, Santa Barbara, California, USA
A. Barzdukas, L. Brennan, C. Campagnari, G. Collura, A. Dorsett, J. Incandela,

M. Kilpatrick, J. Kim, A.J. Li, P. Masterson, H. Mei, M. Oshiro, J. Richman, U. Sarica, R. Schmitz, F. Setti, J. Sheplock, D. Stuart, S. Wang

California Institute of Technology, Pasadena, California, USA
A. Bornheim, O. Cerri, A. Latorre, J.M. Lawhorn, J. Mao, H.B. Newman, T. Q. Nguyen, M. Spiropulu, J.R. Vlimant, C. Wang, S. Xie, R.Y. Zhu

Carnegie Mellon University, Pittsburgh, Pennsylvania, USA
J. Alison, S. An, M.B. Andrews, P. Bryant, V. Dutta, T. Ferguson, A. Harilal, C. Liu, T. Mudholkar, S. Murthy, M. Paulini, A. Roberts, A. Sanchez, W. Terrill

University of Colorado Boulder, Boulder, Colorado, USA
J.P. Cumalat, W.T. Ford, A. Hassani, G. Karathanasis, E. MacDonald, N. Manganelli, F. Marini, A. Perloff, C. Savard, N. Schonbeck, K. Stenson, K.A. Ulmer, S.R. Wagner, N. Zipper

Cornell University, Ithaca, New York, USA
J. Alexander, S. Bright-Thonney, X. Chen, D.J. Cranshaw, J. Fan, X. Fan, D. Gadkari, S. Hogan, J. Monroy, J.R. Patterson, J. Reichert, M. Reid, A. Ryd, J. Thom, P. Wittich, R. Zou

Fermi National Accelerator Laboratory, Batavia, Illinois, USA
M. Albrow, M. Alyari, O. Amram, G. Apollinari, A. Apresyan, L.A.T. Bauerdick, D. Berry, J. Berryhill, P.C. Bhat, K. Burkett, J.N. Butler, A. Canepa, G.B. Cerati, H.W.K. Cheung, F. Chlebana, G. Cummings, J. Dickinson, I. Dutta, V.D. Elvira, Y. Feng, J. Freeman, A. Gandrakota, Z. Gecse, L. Gray, D. Green, A. Grummer, S. Grünendahl, D. Guerrero, O. Gutsche, R.M. Harris, R. Heller, T.C. Herwig, J. Hirschauer, L. Horyn, B. Jayatilaka, S. Jindariani, M. Johnson, U. Joshi, T. Klijnsma, B. Klima, K.H.M. Kwok, S. Lammel, D. Lincoln, R. Lipton, T. Liu, C. Madrid, K. Maeshima, C. Mantilla, D. Mason, P. McBride, P. Merkel, S. Mrenna, S. Nahn, J. Ngadiuba, D. Noonan, V. Papadimitriou, N. Pastika, K. Pedro, C. Pena[87], F. Ravera, A. Reinsvold Hall[88], L. Ristori, E. Sexton-Kennedy, N. Smith, A. Soha, L. Spiegel, S. Stoynev, L. Taylor, S. Tkaczyk, N.V. Tran, L. Uplegger, E.W. Vaandering, I. Zoi

University of Florida, Gainesville, Florida, USA
C. Aruta, P. Avery, D. Bourilkov, L. Cadamuro, P. Chang, V. Cherepanov, R.D. Field, E. Koenig, M. Kolosova, J. Konigsberg, A. Korytov, K.H. Lo, K. Matchev, N. Menendez, G. Mitselmakher, A. Muthirakalayil Madhu, N. Rawal, D. Rosenzweig, S. Rosenzweig, K. Shi, J. Wang

Florida State University, Tallahassee, Florida, USA
T. Adams, A. Al Kadhim, A. Askew, N. Bower, R. Habibullah, V. Hagopian, R. Hashmi, R.S. Kim, S. Kim, T. Kolberg, G. Martinez, H. Prosper, P.R. Prova, O. Viazlo, M. Wulansatiti, R. Yohay, J. Zhang

Florida Institute of Technology, Melbourne, Florida, USA
B. Alsufyani, M.M. Baarmand, S. Butalla, T. Elkafrawy[17], M. Hohlmann, R. Kumar Verma, M. Rahmani

University of Illinois at Chicago (UIC), Chicago, Illinois, USA
M.R. Adams, C. Bennett, R. Cavanaugh, S. Dittmer, R. Escobar Franco, O. Evdokimov, C.E. Gerber, D.J. Hofman, J.h. Lee, D. S. Lemos, A.H. Merrit, C. Mills, S. Nanda, G. Oh, B. Ozek, D. Pilipovic, T. Roy, S. Rudrabhatla, M.B. Tonjes,

N. Varelas, X. Wang, Z. Ye, J. Yoo

The University of Iowa, Iowa City, Iowa, USA
M. Alhusseini, D. Blend, K. Dilsiz[89], L. Emediato, G. Karaman, O.K. Köseyan, J.-P. Merlo, A. Mestvirishvili[90], J. Nachtman, O. Neogi, H. Ogul[91], Y. Onel, A. Penzo, C. Snyder, E. Tiras[92]

Johns Hopkins University, Baltimore, Maryland, USA
B. Blumenfeld, L. Corcodilos, J. Davis, A.V. Gritsan, L. Kang, S. Kyriacou, P. Maksimovic, M. Roguljic, J. Roskes, S. Sekhar, M. Swartz, T.Á. Vámi

The University of Kansas, Lawrence, Kansas, USA
A. Abreu, L.F. Alcerro Alcerro, J. Anguiano, P. Baringer, A. Bean, Z. Flowers, D. Grove, J. King, G. Krintiras, M. Lazarovits, C. Le Mahieu, C. Lindsey, J. Marquez, N. Minafra, M. Murray, M. Nickel, M. Pitt, S. Popescu[93], C. Rogan, C. Royon, R. Salvatico, S. Sanders, C. Smith, Q. Wang, G. Wilson

Kansas State University, Manhattan, Kansas, USA
B. Allmond, A. Ivanov, K. Kaadze, A. Kalogeropoulos, D. Kim, Y. Maravin, K. Nam, J. Natoli, D. Roy, G. Sorrentino

Lawrence Livermore National Laboratory, Livermore, California, USA
F. Rebassoo, D. Wright

University of Maryland, College Park, Maryland, USA
E. Adams, A. Baden, O. Baron, A. Belloni, A. Bethani, Y.M. Chen, S.C. Eno, N.J. Hadley, S. Jabeen, R.G. Kellogg, T. Koeth, Y. Lai, S. Lascio, A.C. Mignerey, S. Nabili, C. Palmer, C. Papageorgakis, M.M. Paranjpe, L. Wang, K. Wong

Massachusetts Institute of Technology, Cambridge, Massachusetts, USA
J. Bendavid, W. Busza, I.A. Cali, Y. Chen, M. D'Alfonso, J. Eysermans, C. Freer, G. Gomez-Ceballos, M. Goncharov, P. Harris, D. Hoang, D. Kovalskyi, J. Krupa, L. Lavezzo, Y.-J. Lee, K. Long, C. Mironov, C. Paus, D. Rankin, C. Roland, G. Roland, S. Rothman, Z. Shi, G.S.F. Stephans, J. Wang, Z. Wang, B. Wyslouch, T. J. Yang

University of Minnesota, Minneapolis, Minnesota, USA
B. Crossman, B.M. Joshi, C. Kapsiak, M. Krohn, D. Mahon, J. Mans, B. Marzocchi, S. Pandey, M. Revering, R. Rusack, R. Saradhy, N. Schroeder, N. Strobbe, M.A. Wadud

University of Mississippi, Oxford, Mississippi, USA
L.M. Cremaldi

University of Nebraska-Lincoln, Lincoln, Nebraska, USA
K. Bloom, M. Bryson, D.R. Claes, C. Fangmeier, F. Golf, J. Hossain, C. Joo, I. Kravchenko, I. Reed, J.E. Siado, G.R. Snow†, W. Tabb, A. Vagnerini, A. Wightman, F. Yan, D. Yu, A.G. Zecchinelli

State University of New York at Buffalo, Buffalo, New York, USA
G. Agarwal, H. Bandyopadhyay, L. Hay, I. Iashvili, A. Kharchilava, C. McLean, M. Morris, D. Nguyen, J. Pekkanen, S. Rappoccio, H. Rejeb Sfar, A. Williams

Northeastern University, Boston, Massachusetts, USA
G. Alverson, E. Barberis, Y. Haddad, Y. Han, A. Krishna, J. Li, M. Lu,

G. Madigan, D.M. Morse, V. Nguyen, T. Orimoto, A. Parker, L. Skinnari, A. Tishelman-Charny, B. Wang, D. Wood

Northwestern University, Evanston, Illinois, USA
S. Bhattacharya, J. Bueghly, Z. Chen, K.A. Hahn, Y. Liu, Y. Miao, D.G. Monk, M.H. Schmitt, A. Taliercio, M. Velasco

University of Notre Dame, Notre Dame, Indiana, USA
R. Band, R. Bucci, S. Castells, M. Cremonesi, A. Das, R. Goldouzian, M. Hildreth, K.W. Ho, K. Hurtado Anampa, C. Jessop, K. Lannon, J. Lawrence, N. Loukas, L. Lutton, J. Mariano, N. Marinelli, I. Mcalister, T. McCauley, C. Mcgrady, K. Mohrman, C. Moore, Y. Musienko[13], H. Nelson, M. Osherson, R. Ruchti, A. Townsend, M. Wayne, H. Yockey, M. Zarucki, L. Zygala

The Ohio State University, Columbus, Ohio, USA
A. Basnet, B. Bylsma, M. Carrigan, L.S. Durkin, C. Hill, M. Joyce, A. Lesauvage, M. Nunez Ornelas, K. Wei, B.L. Winer, B. R. Yates

Princeton University, Princeton, New Jersey, USA
F.M. Addesa, H. Bouchamaoui, P. Das, G. Dezoort, P. Elmer, A. Frankenthal, B. Greenberg, N. Haubrich, S. Higginbotham, G. Kopp, S. Kwan, D. Lange, A. Loeliger, D. Marlow, I. Ojalvo, J. Olsen, D. Stickland, C. Tully

University of Puerto Rico, Mayaguez, Puerto Rico, USA
S. Malik

Purdue University, West Lafayette, Indiana, USA
A.S. Bakshi, V.E. Barnes, S. Chandra, R. Chawla, S. Das, A. Gu, L. Gutay, M. Jones, A.W. Jung, D. Kondratyev, A.M. Koshy, M. Liu, G. Negro, N. Neumeister, G. Paspalaki, S. Piperov, A. Purohit, J.F. Schulte, M. Stojanovic, J. Thieman, A. K. Virdi, F. Wang, W. Xie

Purdue University Northwest, Hammond, Indiana, USA
J. Dolen, N. Parashar, A. Pathak

Rice University, Houston, Texas, USA
D. Acosta, A. Baty, T. Carnahan, S. Dildick, K.M. Ecklund, P.J. Fernández Manteca, S. Freed, P. Gardner, F.J.M. Geurts, A. Kumar, W. Li, O. Miguel Colin, B.P. Padley, R. Redjimi, J. Rotter, E. Yigitbasi, Y. Zhang

University of Rochester, Rochester, New York, USA
A. Bodek, P. de Barbaro, R. Demina, J.L. Dulemba, C. Fallon, A. Garcia-Bellido, O. Hindrichs, A. Khukhunaishvili, P. Parygin[83], E. Popova[83], R. Taus, G.P. Van Onsem

The Rockefeller University, New York, New York, USA
K. Goulianos

Rutgers, The State University of New Jersey, Piscataway, New Jersey, USA
B. Chiarito, J.P. Chou, Y. Gershtein, E. Halkiadakis, A. Hart, M. Heindl, D. Jaroslawski, O. Karacheban[28], I. Laflotte, A. Lath, R. Montalvo, K. Nash, H. Routray, S. Salur, S. Schnetzer, S. Somalwar, R. Stone, S.A. Thayil, S. Thomas, J. Vora, H. Wang

University of Tennessee, Knoxville, Tennessee, USA

H. Acharya, D. Ally, A.G. Delannoy, S. Fiorendi, T. Holmes, N. Karunarathna, L. Lee, E. Nibigira, S. Spanier

Texas A&M University, College Station, Texas, USA
D. Aebi, M. Ahmad, O. Bouhali[94], M. Dalchenko, R. Eusebi, J. Gilmore, T. Huang, T. Kamon[95], H. Kim, S. Luo, S. Malhotra, R. Mueller, D. Overton, D. Rathjens, A. Safonov

Texas Tech University, Lubbock, Texas, USA
N. Akchurin, J. Damgov, V. Hegde, A. Hussain, Y. Kazhykarim, K. Lamichhane, S.W. Lee, A. Mankel, T. Mengke, S. Muthumuni, T. Peltola, I. Volobouev, A. Whitbeck

Vanderbilt University, Nashville, Tennessee, USA
E. Appelt, S. Greene, A. Gurrola, W. Johns, R. Kunnawalkam Elayavalli, A. Melo, F. Romeo, P. Sheldon, S. Tuo, J. Velkovska, J. Viinikainen

University of Virginia, Charlottesville, Virginia, USA
B. Cardwell, B. Cox, J. Hakala, R. Hirosky, A. Ledovskoy, A. Li, C. Neu, C.E. Perez Lara

Wayne State University, Detroit, Michigan, USA
P.E. Karchin

University of Wisconsin - Madison, Madison, Wisconsin, USA
A. Aravind, S. Banerjee, K. Black, T. Bose, S. Dasu, I. De Bruyn, P. Everaerts, C. Galloni, H. He, M. Herndon, A. Herve, C.K. Koraka, A. Lanaro, R. Loveless, J. Madhusudanan Sreekala, A. Mallampalli, A. Mohammadi, S. Mondal, G. Parida, D. Pinna, A. Savin, V. Shang, V. Sharma, W.H. Smith, D. Teague, H.F. Tsoi, W. Vetens, A. Warden

Authors affiliated with an institute or an international laboratory covered by a cooperation agreement with CERN
S. Afanasiev, V. Andreev, Yu. Andreev, T. Aushev, M. Azarkin, A. Babaev, A. Belyaev, V. Blinov[96], E. Boos, V. Borshch, D. Budkouski, V. Bunichev, V. Chekhovsky, R. Chistov[96], M. Danilov[96], A. Dermenev, T. Dimova[96], D. Druzhkin[97], M. Dubinin[87], L. Dudko, A. Ershov, G. Gavrilov, V. Gavrilov, S. Gninenko, V. Golovtcov, N. Golubev, I. Golutvin, I. Gorbunov, Y. Ivanov, V. Kachanov, L. Kardapoltsev[96], V. Karjavine, A. Karneyeu, V. Kim[96], M. Kirakosyan, D. Kirpichnikov, M. Kirsanov, V. Klyukhin, D. Konstantinov, V. Korenkov, A. Kozyrev[96], N. Krasnikov, A. Lanev, P. Levchenko[98], N. Lychkovskaya, V. Makarenko, A. Malakhov, V. Matveev[96], V. Murzin, A. Nikitenko[99,100], S. Obraztsov, V. Oreshkin, V. Palichik, V. Perelygin, M. Perfilov, S. Petrushanko, S. Polikarpov[96], V. Popov, O. Radchenko[96], M. Savina, V. Savrin, V. Shalaev, S. Shmatov, S. Shulha, Y. Skovpen[96], S. Slabospitskii, V. Smirnov, A. Snigirev, D. Sosnov, V. Sulimov, E. Tcherniaev, A. Terkulov, O. Teryaev, I. Tlisova, A. Toropin, L. Uvarov, A. Uzunian, P. Volkov, A. Vorobyev†, N. Voytishin, B.S. Yuldashev[101], A. Zarubin, I. Zhizhin, A. Zhokin

†: Deceased
[1]Also at Yerevan State University, Yerevan, Armenia
[2]Also at TU Wien, Vienna, Austria
[3]Also at Institute of Basic and Applied Sciences, Faculty of Engineering, Arab Academy for

Science, Technology and Maritime Transport, Alexandria, Egypt
[4]Also at Ghent University, Ghent, Belgium
[5]Also at Universidade Estadual de Campinas, Campinas, Brazil
[6]Also at Federal University of Rio Grande do Sul, Porto Alegre, Brazil
[7]Also at UFMS, Nova Andradina, Brazil
[8]Also at Nanjing Normal University Department of Physics, Nanjing, China
[9]Now at Henan Normal University, Xinxiang, China
[10]Now at The University of Iowa, Iowa City, Iowa, USA
[11]Also at University of Chinese Academy of Sciences, Beijing, China
[12]Also at University of Chinese Academy of Sciences, Beijing, China
[13]Also at an institute or an international laboratory covered by a cooperation agreement with CERN
[14]Also at Helwan University, Cairo, Egypt
[15]Now at Zewail City of Science and Technology, Zewail, Egypt
[16]Also at British University in Egypt, Cairo, Egypt
[17]Now at Ain Shams University, Cairo, Egypt
[18]Also at Birla Institute of Technology, Mesra, Mesra, India
[19]Also at Purdue University, West Lafayette, Indiana, USA
[20]Also at Université de Haute Alsace, Mulhouse, France
[21]Also at Department of Physics, Tsinghua University, Beijing, China
[22]Also at The University of the State of Amazonas, Manaus, Brazil
[23]Also at Erzincan Binali Yildirim University, Erzincan, Turkey
[24]Also at University of Hamburg, Hamburg, Germany
[25]Also at RWTH Aachen University, III. Physikalisches Institut A, Aachen, Germany
[26]Also at Isfahan University of Technology, Isfahan, Iran
[27]Also at Bergische University Wuppertal (BUW), Wuppertal, Germany
[28]Also at Brandenburg University of Technology, Cottbus, Germany
[29]Also at Forschungszentrum Jülich, Juelich, Germany
[30]Also at CERN, European Organization for Nuclear Research, Geneva, Switzerland
[31]Also at Physics Department, Faculty of Science, Assiut University, Assiut, Egypt
[32]Also at Wigner Research Centre for Physics, Budapest, Hungary
[33]Also at Institute of Physics, University of Debrecen, Debrecen, Hungary
[34]Also at Institute of Nuclear Research ATOMKI, Debrecen, Hungary
[35]Now at Universitatea Babes-Bolyai - Facultatea de Fizica, Cluj-Napoca, Romania
[36]Also at Faculty of Informatics, University of Debrecen, Debrecen, Hungary
[37]Also at Punjab Agricultural University, Ludhiana, India
[38]Also at UPES - University of Petroleum and Energy Studies, Dehradun, India
[39]Also at University of Visva-Bharati, Santiniketan, India
[40]Also at University of Hyderabad, Hyderabad, India
[41]Also at Indian Institute of Science (IISc), Bangalore, India
[42]Also at IIT Bhubaneswar, Bhubaneswar, India
[43]Also at Institute of Physics, Bhubaneswar, India
[44]Also at Deutsches Elektronen-Synchrotron, Hamburg, Germany
[45]Also at Department of Physics, Isfahan University of Technology, Isfahan, Iran
[46]Also at Sharif University of Technology, Tehran, Iran
[47]Also at Department of Physics, University of Science and Technology of Mazandaran, Behshahr, Iran
[48]Also at Italian National Agency for New Technologies, Energy and Sustainable Economic Development, Bologna, Italy

[49]Also at Centro Siciliano di Fisica Nucleare e di Struttura Della Materia, Catania, Italy
[50]Also at Università degli Studi Guglielmo Marconi, Roma, Italy
[51]Also at Scuola Superiore Meridionale, Università di Napoli 'Federico II', Napoli, Italy
[52]Also at Fermi National Accelerator Laboratory, Batavia, Illinois, USA
[53]Also at Università di Napoli 'Federico II', Napoli, Italy
[54]Also at Consiglio Nazionale delle Ricerche - Istituto Officina dei Materiali, Perugia, Italy
[55]Also at Riga Technical University, Riga, Latvia
[56]Also at Department of Applied Physics, Faculty of Science and Technology, Universiti Kebangsaan Malaysia, Bangi, Malaysia
[57]Also at Consejo Nacional de Ciencia y Tecnología, Mexico City, Mexico
[58]Also at Trincomalee Campus, Eastern University, Sri Lanka, Nilaveli, Sri Lanka
[59]Also at INFN Sezione di Pavia, Università di Pavia, Pavia, Italy
[60]Also at National and Kapodistrian University of Athens, Athens, Greece
[61]Also at Ecole Polytechnique Fédérale Lausanne, Lausanne, Switzerland
[62]Also at University of Vienna Faculty of Computer Science, Vienna, Austria
[63]Also at Universität Zürich, Zurich, Switzerland
[64]Also at Stefan Meyer Institute for Subatomic Physics, Vienna, Austria
[65]Also at Laboratoire d'Annecy-le-Vieux de Physique des Particules, IN2P3-CNRS, Annecy-le-Vieux, France
[66]Also at Near East University, Research Center of Experimental Health Science, Mersin, Turkey
[67]Also at Konya Technical University, Konya, Turkey
[68]Also at Izmir Bakircay University, Izmir, Turkey
[69]Also at Adiyaman University, Adiyaman, Turkey
[70]Also at Necmettin Erbakan University, Konya, Turkey
[71]Also at Bozok Universitetesi Rektörlügü, Yozgat, Turkey
[72]Also at Marmara University, Istanbul, Turkey
[73]Also at Milli Savunma University, Istanbul, Turkey
[74]Also at Kafkas University, Kars, Turkey
[75]Also at Hacettepe University, Ankara, Turkey
[76]Also at Istanbul University - Cerrahpasa, Faculty of Engineering, Istanbul, Turkey
[77]Also at Yildiz Technical University, Istanbul, Turkey
[78]Also at Vrije Universiteit Brussel, Brussel, Belgium
[79]Also at School of Physics and Astronomy, University of Southampton, Southampton, United Kingdom
[80]Also at University of Bristol, Bristol, United Kingdom
[81]Also at IPPP Durham University, Durham, United Kingdom
[82]Also at Monash University, Faculty of Science, Clayton, Australia
[83]Now at an institute or an international laboratory covered by a cooperation agreement with CERN
[84]Also at Università di Torino, Torino, Italy
[85]Also at Bethel University, St. Paul, Minnesota, USA
[86]Also at Karamanoğlu Mehmetbey University, Karaman, Turkey
[87]Also at California Institute of Technology, Pasadena, California, USA
[88]Also at United States Naval Academy, Annapolis, Maryland, USA
[89]Also at Bingol University, Bingol, Turkey
[90]Also at Georgian Technical University, Tbilisi, Georgia
[91]Also at Sinop University, Sinop, Turkey
[92]Also at Erciyes University, Kayseri, Turkey

[93]Also at Horia Hulubei National Institute of Physics and Nuclear Engineering (IFIN-HH), Bucharest, Romania
[94]Also at Texas A&M University at Qatar, Doha, Qatar
[95]Also at Kyungpook National University, Daegu, Korea
[96]Also at another institute or international laboratory covered by a cooperation agreement with CERN
[97]Also at Universiteit Antwerpen, Antwerpen, Belgium
[98]Also at Northeastern University, Boston, Massachusetts, USA
[99]Also at Imperial College, London, United Kingdom
[100]Now at Yerevan Physics Institute, Yerevan, Armenia
[101]Also at Institute of Nuclear Physics of the Uzbekistan Academy of Sciences, Tashkent, Uzbekistan